

Fracton physics of spatially extended excitations

Meng-Yuan Li and Peng Ye*

School of Physics, Sun Yat-sen University, Guangzhou, 510275, China

(Dated: Friday 29th May, 2020)

Fracton topological order hosts fractionalized point-like excitations (e.g., fractons) that have restricted mobility. In this article, we explore even more bizarre realization of fracton phases that admit spatially extended excitations with restriction on both mobility and deformability. First, we present exactly solvable lattice quantum frustrated spin models and study their ground states and excited states analytically. We construct a family tree in which parent models and descendent models share excitation DNA. Second, with the help of solvability and novel excitation spectrum of these models, we initiate the first-step of general discussions on quantitative and qualitative properties of spatially extended excitations whose mobility and deformability are restricted to some extent. Especially, as a useful viewpoint for understanding such fracton-physics, all excitations are divided into four mutually distinct sectors, namely, simple excitations, complex excitations, intrinsically disconnected excitations, and trivial excitations. Several implications in, e.g., condensed matter physics and gravity are briefly discussed.

CONTENTS

I. Introduction	1	B. Family tree	16
A. Mobility and deformability	1	C. Simple excitations in the model-[0, 1, 2, 4] and [1, 2, 3, 5]	17
B. Sectorization of Hilbert space	3	D. Complex excitations in the model-[1, 2, 3, 5] (“chairon”, “cloverion” and “xunon”)	18
C. Exactly solvable models	4	V. Concluding remarks	19
D. Outline	5	Acknowledgments	19
II. Preliminaries of geometric notations	5	References	19
A. Coordinate system and definition of n -cube	5		
B. Leaf spaces associated with a given cube	5		
C. Definition of “nearest” via L_1 -norm and L_1 -distance	7		
D. Stacking of cubes: straight string, flat membrane, and beyond	7		
III. $[D - 3, D - 2, D - 1, D]$ model series	7		
A. Construction of $[D - 3, D - 2, D - 1, D]$ models	7		
B. The X-cube model as $[0, 1, 2, 3]$	8		
C. Simple excitations in the model-[1, 2, 3, 4]	9		
1. (0, 0)-type point-like excitations (fractons)	10		
2. (0, 3)-type point-like excitations (connected volumeons)	10		
3. (1, 2)-type string excitations of 6 flavors	11		
D. Complex excitations in the model-[1, 2, 3, 4]	13		
1. Chairons of 12 flavors	13		
2. Yuons of 4 flavors	13		
E. Excited states with multiple spatially separate loops in the model-[1, 2, 3, 4]	14		
F. Gravity analog: energy density and spacetime curvature	14		
IV. General construction of lattice models	15		
A. Lattice Hamiltonians	15		

I. INTRODUCTION

A. Mobility and deformability

Hunting for unconventional orders—beyond symmetry-breaking orders—is one of missions of modern condensed matter physicists. One of popular examples of unconventional orders is topological order that supports nontrivial topological excitations, e.g., anyons in the fractional quantum Hall effect [1, 2]. The creation and annihilation quantum operator of a single topological excitation in the bulk, e.g., e particle in toric code model, must be nonlocal. This nonlocality also leads to robustness of topological order against local perturbations, partially forming the argument on robustness of topological quantum computation[3]. Meanwhile, proper local operators can be constructed to spatially move a topological excitation. Even in a tight-binding model, a “topologically trivial” electron can locally hop from site- j to site- i under the local operator $\sim c_i^\dagger c_j$. This property is “free mobility”. Recently, the invalidity of this seemingly obvious property has been found in a class of many-body systems that support topological excitations called “fractons” [4, 5]. If one tries to move a fracton, extra fractons will be created nearby, causing unfavorable energy penalty. Quantum mechanically, the mobility restriction is deeply rooted in the lack of local

* yepeng5@mail.sysu.edu.cn

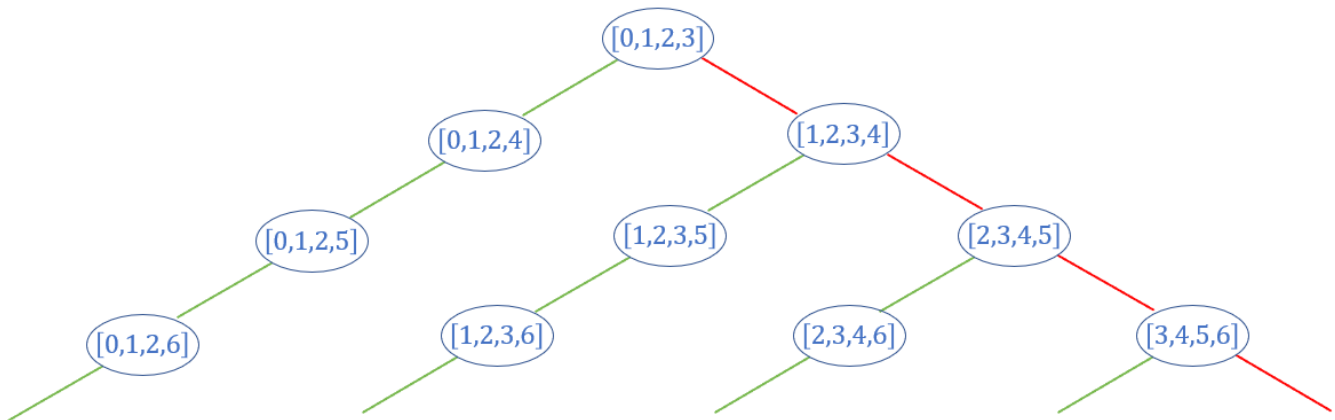


FIG. 1. The family tree of exactly solvable fracton models in all dimensions. The models are labeled by 4 dimension indexes, which will be introduced in Sec. IV A. Considering that a model may share a lot of similarities with a lower dimensional model, a part of exactly solvable models can be organized in a tree diagram. Here every straight line (in either green or red) links a low dimensional parent model and a high dimensional descendant model. In general, a descendant model may share some “excitation DNA” with its parent model. For example, a red line means the $(i, i + 1)$ -type excitations in the parent model are promoted to $(i + 1, i + 2)$ -type excitations in the descendant model (as we shall exemplify in Table. II). Even though, due to the existence of \mathbf{E}^c excitations, the spectrum of a model can still be quite unpredictable, as we shall demonstrate in the following sections.

operators that act on a one-fracton excited state by *merely* changing the fracton’s location. There are two issues about lack-of-mobility to be clarified. First, in some sense, this lack of mobility in absence of external disorders and impurities is more or less similar to the concept of self-localization phenomenon although the latter arises in some other strongly-correlated systems, e.g., in Ref. [6], via very different microscopic origins. Second, lack of mobility leads to flat energy dispersion relation, but flat energy dispersion relation is insufficient for defining a *fracton phase*. All excitations in the \mathbb{Z}_2 topological order fixed-point “toric code model” have flat dispersion but all excitations can be locally moved.

Surprisingly, such stringent restriction on mobility did not trivialize underlying physics at all. On the contrary, it has been discovered that mobility restriction leads to unexpectedly rich quantum phenomena of many-body physics, dubbed “*fracton-physics*”. For example, in some exactly solvable models, ground state degeneracy (GSD) is not only topological but also dependent on the system size! More specifically, GSD of some models [7] may grow exponentially with respect to the length/width/height of 3D systems, while, mutually orthogonal degenerate ground states are strictly indistinguishable under any local measurements. Generally speaking, such many-body systems possess a part of intrinsic defining properties of *pure topological order*¹ but the thermodynamical limit of these systems turns out to be quite subtle

and unusual. Such an “unconventional” type of topological order, dubbed “*fracton topological order*” represents a brand-new line of thinking about strongly-correlated topological phases of matter, and has been gaining much attention recently. Researchers have successfully made connection between fracton-physics and vast subfields of theoretical physics, including glassy dynamics, foliation theory, elasticity, dipole algebra, higher-rank global symmetry, many-body localization, stabilizer codes, duality, gravity, quantum spin liquid, and higher-rank gauge theory [4, 5, 7–45]. Some of these subfields, from previous points of view, seem no doubt “orthogonal” to each other! Being topically related to the present article, exactly solvable lattice models in the literature (e.g., [5, 10–21, 25, 46]) have been reported in 3D lattice quantum frustrated spin models of type-I and type-II. In type-I series, e.g, the X-cube model [5], the low-lying excitation spectrum supports both fractons and “subdimensional particles” whose mobility is free only inside a subspace (e.g., straight lines formed by links and flat plane formed by faces of dual lattice) of 3D cubic lattice. On the contrary, in type-II series, e.g., the Haah’s code [12], all topological excitations are fractons. For readers who are interested but unfamiliar with the rapid progress in the field of fracton-physics, an up-to-date review in Ref. [47] is recommended.

Currently, the main stream on the topic of fracton topological order focuses on particle excitations which are point-like². Nevertheless, in addition to particles, being a striking theoretical progress in condensed matter physics,

¹ Hereafter, for avoiding confusion of terminologies, we use “pure topological order” to denote the well-known concept “topological order” [1, 2].

² Just like pure topological order, the geometric shapes of excitations can be properly defined by using continuous spacetime

spatially extended excitations, e.g., string and membrane excitations, have been systematically constructed in 3D and higher dimensional pure topological order [48]. It should be kept in mind that, higher-dimensional pure topological order has been analyzed towards a unified mathematical framework [49–51]. In the presence of spatially extended excitations, plentiful quantum phenomena and microscopic justification have been reported analytically, such as exotic entanglement, symmetry enrichment, adiabatic braiding statistics and topological quantum field theory, and higher-category [49, 50, 52–73]. *Therefore, it is quite valuable to move forward to explore underlying physics of spatially extended excitations that cannot freely move and deform.* With the preparation and interests from both pure topological order side and fracton-physics side, it is time to make efforts to study the highly unexplored marriage of spatially extended excitations and mobility/deformability restriction. Despite less progress compared to particle excitations, to the best of our knowledge, there has been one intriguing field-theoretical analysis on “*fractonic lines*” in Ref. [40], i.e., completely immobile strings. It was claimed that, the presence of such exotic excitations is tightly related to sophisticated higher-rank gauge theory and potentially beneficial to quantum error-correction and quantum storage.

The main results of this article can be summarized in two aspects. *First, we present exactly solvable lattice quantum frustrated spin models in three and higher dimensions $D \geq 3$.* All models reduce to the aforementioned X-cube model once dimensions are lowered to 3D. But for the definite space dimensions higher than 3D, there are more than one models. All models form a hierarchical structure of model Hamiltonians. Some representative series of models are illustrated in Fig. 1 since *a part of* excitations in these models obey simple dimension reduction rules. In these models, topologically excited states contain not only fractonic strings [40], but also more complex varieties as to be discussed in the main text. *Second, motivated by these models, we initiate the first-step of general discussions on spatially extended excitations whose mobility and deformability are restricted to some extent. Both qualitative and quantitative properties in such exotic fracton physics will be discussed.* Along this line of thinking, one challenging problem is to characterize and classify topological excitations based on mobility and deformability against local operators. Pictorially, a spatially extended object in classical mechanics may leave its original position via either *rigid translation* or *elastic deformation*. To measure the ability of realizing these two processes, we introduce respectively “mo-

only after smoothing lattice. For example, m particle in the toric code model on a square lattice is actually labeled by a plaquette operator whose eigenvalue is flipped, but can be regarded as a point-like object once the background lattice is smoothen. It also means that all geometric structures below the lattice spacing are invisible.

bility” and “deformability” as mentioned above. Such a classical scenario looks more complicated than point-like excitations, which motivates us to carefully examine how excitations are deformed and moved under local quantum operators.

Before moving on, we provide some justification for models in dimensions higher than the physically relevant dimensions of three. Traditionally, it is meaningful to study condensed matter systems only in dimensions of one, two, and three. It seems unreasonable to go beyond. Nevertheless, research in all dimensions has been very common, especially in the field of topological phases of matter. Organizational principles or mathematical structures of topological phases of matter are often unveiled during the systematic treatment via varying dimensions. For example, the periodic table of free-fermion gapped states with symmetry shows interesting periodic behaviors when increasing space dimensions topological insulators, by the procedure of dimensional reduction [74–77]. In the group-cohomology construction of bosonic symmetry-protected topological phases (SPT), SPTs in higher dimensions can be constructed by SPTs in lower dimensions via Künneth formula of cohomology theory [78, 79], which is physically discussed via the “*decoration scenario*”. Also in SPTs, there exist exotic dimension-dependent patterns for general response theories of bosonic integer quantum Hall states in all even (spatial) dimensions and bosonic topological insulators in all odd (spatial) dimensions [80]. There are also interesting discussions on anomalous topological phases of matter in 3D [63, 65, 81, 82]. Quantum anomaly of these states is expected to be canceled by 4D bulk states. [83] studies how to realize interacting topological insulators with synthetic dimensions and [84] proposes a 4D exactly solvable SPT model beyond cohomology. The last example is the general theory of topological order in all dimensions [51] which has also been mentioned above.

B. Sectorization of Hilbert space

Among many properties of spatially extended excitations, in this article, we focus on mobility and deformability under local operators. In the long-wavelength limit, we demand that the size of spatially extended excitations is sufficiently large compared to correlation length. All local operators are supported in the space whose size is much smaller than the excitation size such that topology of configuration space in the presence of excitations (e.g., defects) keeps unaltered under local operators. We find that the Hilbert space of models that support fracton topological order can be divided into four sectors, as shown in Fig. 2. \mathbb{I} incorporates all trivial excited states e.g., local spin flipping, including ground states themselves as well. Trivial excitations can be created by local operators above the ground states. The remaining three sectors are three mutually distinct classes of topological excitations: *simple excitations* E^s , *complex excitations*

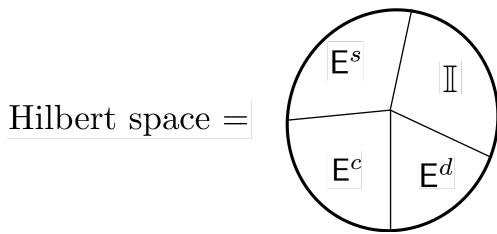


FIG. 2. Sectorization of Hilbert space. It is guaranteed that two excitations belonging to two different sectors definitely cannot be changed to each other by any local operators.

E^c and (*intrinsically*) *disconnected excitations* E^d . Below we shall define E^s, E^c, E^d .

Let us first assume geometric shape of excitations is connected. At infrared scales where lattice has been smoothen (see footnote 2), simple excitations denoted by E^s have manifold-like shape, e.g., point-like, string-like, membrane-like. All these excitations, once withdrawing the restriction on mobility and deformability, can appear in pure topological order [49, 50]. Mathematically, all these geometric structures can be locally regarded as a n -dimensional Euclidean space (see Page 219 of Ref. [85]), where $n = 0$ for points (i.e., particles), $n = 1$ for strings, $n = 2$ for membranes, \dots . In order to characterize simple excitations in a unified framework, in the present article, we introduce a pair of integers (n, m) . Here, m denotes the dimension of the subspace where excitations can freely move and deform³. Therefore, fractons are simply labeled by $(0, 0)$. Likewise, a string excitation whose mobility and deformability are allowed within a plane is a $(1, 2)$ -type excitation. Obviously, if $m = D$, then such excitations are actually mobile and deformable in the whole D -dimensional space, which exactly covers all excitations in pure topological order.

On the other hand, for complex excitations denoted by E^c , physical properties of both geometric shapes and mobility are entirely different from the above description of simple excitations. The physical characterization (e.g., creation operators, excitation energy, fusion rules, mobility) is far more intricate than that of simple excitations. When we consider the connected configurations of excitations, the shapes of complex excitations can only be non-manifold-like [85], so a pair of number (n, m) is no longer a good label. And consequently, the description of mobility and deformability becomes more complicated. But it is definite that any point-like excitations cannot belong to E^c since a point is always a manifold. The first example of E^c that we will introduce in the main text is

³ Obviously, m is insufficient to uniquely label a general subspace. For example, it is reasonable to consider a model where a string excitation is movable and deformable inside a certain solid torus. Nevertheless, we only focus on the simplest situation: for dimension- m , the subspace is a stacking of infinite parallel *straight* lines ($m = 1$), *flat* planes ($m = 2$), \dots .

dubbed “chairon” due to its “legless chair-like” shape as shown in Fig. 7(b). More complicated examples such as “yuons”, “xuons” and “cloverions” will be discussed in the main text associated with Fig. 8 and Fig. 10.

Simple excitations and complex excitations defined above are restricted to geometrically connected shapes. Nevertheless, we should naturally generalize these definitions in order to incorporate some excited states with disconnected pieces. For disconnected shapes, excitations (more precisely “excited states”) can be divided into two subclasses: E^d and \tilde{E}^d . The shapes of all excitations in E^d are said to be “intrinsically disconnected”: there is no way to fuse disconnected pieces to connected shapes due to restrictions of mobility and deformability. To some extent, the existence of E^d is a hallmark of fracton topological order. On the contrary, all excitations in \tilde{E}^d can always be fused into excitations with connected shapes of either manifold-like or non-manifold-like⁴. In this sense, all excitations in \tilde{E}^d can be fully covered by either \mathbb{I} , E^s or E^c . If non-manifold-like shape is the *only* option of fusions, the excitation with disconnected shape is said to be in E^c sector. In short, we do not separately consider \tilde{E}^d in Fig. 2. Applying this sectorization of Hilbert space to the three-dimensional X-cube model can be found in Sec. III B.

In summary, the Hilbert space (eigenstate spectrum) can be divided into four sectors. In a certain sector, all excitations, after being moved and deformed by arbitrary local operators, always stay inside the sector. In other words, it is impossible to change one excitation in a given sector, via local operators, to another excitation in another sector. We will see in this article, this sectorization scheme is very useful in fracton-physics of spatially extended excitations.

C. Exactly solvable models

In the main text of this article, we discuss the fracton physics of spatially extended excitations through exactly solvable models. Since there are some additional tunable degrees of freedom within the same spatial dimension D , we find that at least four dimension indices (note: D is included) are necessary to label a model. In the following part of this article, we will use a tuple $[d_n, d_s, d_l, D]$ with a series of constraints required by exact solvability conditions. Technical details of each integer will be given in the main text. For $D = 3$, $[0, 1, 2, 3]$ is the only model that is exact solvable. In fact, this 3D model is nothing but the standard X-cube model [8].

While there are usually more than one models for a more general D , we first pick a typical model series— $[D - 3, D - 2, D - 1, D]$ —to systematically unveil ex-

⁴ In this article, we only consider the simplest fusion process: output channel is unique.

otic properties of spatially extended excitations with restricted mobility and deformability. The model-[0, 1, 2, 4] has similar simple excitation contents as 3D X-cube model. But the model-[1, 2, 3, 4] supports a very fruitful topological excitation spectrum with all three non-trivial sectors, which will be studied in details in the main text. Some other models, such as [1, 2, 3, 5] will also be studied in which chairons, xuons and cloverions are found. We finally provide a family tree in Fig. 1 to summarize some models that share similar properties of excitations. Several interesting rules are found and summarized as a family tree according to the relation of excitation spectrum between parent models and descendent models (see the caption for details).

Some examples are summarized in Table I. It is obvious from the table that pure topological order only supports topological excitations in E^s with the label $(n, m) = (n, D)$. For example, in pure topological order represented by 3D toric code model, point-like and string-like excitations are labeled by (0, 3) and (1, 3) respectively, both of which belong to E^s sector. On the other hand, fracton topological order support more than that. X-cube model supports topological excitations of E^s and E^d sectors while some models constructed in this article support all possible sectors.

D. Outline

The remainder of this article is organized as follows. In Sec. II, we introduce geometric notations that are necessary to symbolize derivations in hyper-cubic lattices. With the help of these notations, all derivations are transformed into a computable algebraic way.

In Sec. III, we discuss a series of models called “[$D - 3, D - 2, D - 1, D$] models”. A general introduction of the series is given in Sec. III A, while the X-cube model introduced in Sec. III B has been naturally incorporated in this series and labeled by [0, 1, 2, 3]. For beginners of fracton-physics, it is highly recommended to go through the X-cube model where some notations and physics are useful for later discussions. In Sec. III C and Sec. III D, we work out the model-[1, 2, 3, 4] that exemplifies the construction of spatially extended excitations of both “simple” and “complex” categories. In this model, simple excitations are composed by fractons labeled by (0, 0), volumeons labeled by (0, 3), and strings labeled by (1, 2) with 6 flavors. Complex excitations of this model are chairons and yuons. Considering that in pure topological orders excited states with separated loops are rarely discussed, Sec. III E is devoted to a detailed discussion of such states, as now they are of great importance to understand the bizarre behavior of [$D - 3, D - 2, D - 1, D$] models. The construction of general $(i, i + 1)$ -type excitations and its possible relationship with gravity is also presented in Sec. III F.

In Sec. IV, we present a general procedure to produce a whole class of exactly solvable lattice models for fracton

topological order in all dimensions $D \geq 3$. Each model is labeled by four integers [d_n, d_s, d_l, D], which means that the above model series [$D - 3, D - 2, D - 1, D$] is just a tip of iceberg of model family. The construction and general discussion of the whole model family is presented in Sec. IV A, and a family tree based on similarity of excitation spectrum is drawn in Fig. 1 in Sec. IV B. In Sec. IV C and Sec. IV D we concretely discuss the model-[1, 2, 3, 5], while the model-[0, 1, 2, 4] is also discussed briefly in Sec. IV C. Many examples of complex excitations, like β -chairons, cloverions and xuons are analyzed in details.

Sec. V is devoted to concluding remarks. Several related problems are presented for the future investigation.

II. PRELIMINARIES OF GEOMETRIC NOTATIONS

A. Coordinate system and definition of n -cube

In this article, we’re mainly interested in the high dimensional models, so it’s highly desirable to define and unify a group of notations for describing high dimensional objects. First, we introduce “ n -cube”. It is n -dimensional analog of a common “cube”, and we use the symbol γ_n to denote an n -cube. Some simple examples are shown in Fig. 3. In other words, 0-cube, 1-cube and 2-cube are respectively a lattice site, a link and a plaquette. Without loss of generality, we set the hypercubic lattice with periodic boundary condition to be D -dimensional with lattice constant $a = 1$. Therefore, we can refer to every n -cube in the lattice by a unique Cartesian coordinate, *which is the coordinate of the geometric center of γ_n* . Obviously, the coordinate representation of γ_n is composed by n half-integers and $(D - n)$ integers. For example, a usual vertex is a 0-cube. In the remainder of this article, we may simply use the coordinate of an n -cube to refer to the n -cube itself, since the coordinate can uniquely label an n -cube.

In D -dimensional lattice, there are D orthogonal directions: $\hat{x}_1, \hat{x}_2, \dots, \hat{x}_D$. For a specific $\gamma_{d_n} = (x_1, x_2, \dots, x_D)$, the set $\mathcal{C}_{\gamma_{d_n}}^i$ is a collection of $(D - d_n)$ orthogonal directions along which the coordinates of γ_{d_n} are integer-valued. Likewise, the set $\mathcal{C}_{\gamma_{d_n}}^h$ is composed by d_n directions along which γ_{d_n} has half-integer coordinates. For example, in 3D cubic lattice, for plaquette (i.e. 2-cube) $\gamma_2 = (\frac{1}{2}, \frac{1}{2}, 0)$, we have $\mathcal{C}_{\gamma_2}^i = \{\hat{x}_3\}$ and $\mathcal{C}_{\gamma_2}^h = \{\hat{x}_1, \hat{x}_2\}$.

B. Leaf spaces associated with a given cube

In addition to the notion of n -cube, we also introduce a useful subspace, namely, d_l -dimensional leaf space associated with a given γ_{d_n} . By “associated”, we mean that the γ_{d_n} must be fully embedded in the leaf space l , and $d_l > d_n$ is assumed. Symbolically, we use $l =$

TABLE I. Excitations sectors of different models. More details about the excitations in the listed models are respectively given in Table. IV, Table. VI, Table. VII and Table. VIII. \checkmark and \times denote existence and nonexistence respectively.

Exactly solvable models	\mathbb{I}	\mathbb{E}^s	\mathbb{E}^d	\mathbb{E}^c
SPT (e.g., cohomological models)	\checkmark	\times	\times	\times
Pure topological orders (e.g., 3D toric code models)	\checkmark	\checkmark	\times	\times
X-cube model $([0, 1, 2, 3])$	\checkmark	\checkmark	\checkmark	\times
$[1, 2, 3, 4]$	\checkmark	\checkmark	\checkmark	\checkmark
$[0, 1, 2, 4]$	\checkmark	\checkmark	\checkmark	\times
$[1, 2, 3, 5]$	\checkmark	\checkmark	\checkmark	\checkmark
$[0, 1, 4, 5]$	\checkmark	\checkmark	\checkmark	\times
$[0, 2, 4, 5]$	\checkmark	\checkmark	\checkmark	\times
$[0, 3, 4, 5]$	\checkmark	\checkmark	\checkmark	\times
$[2, 3, 4, 5]$	\checkmark	\checkmark	\checkmark	\checkmark

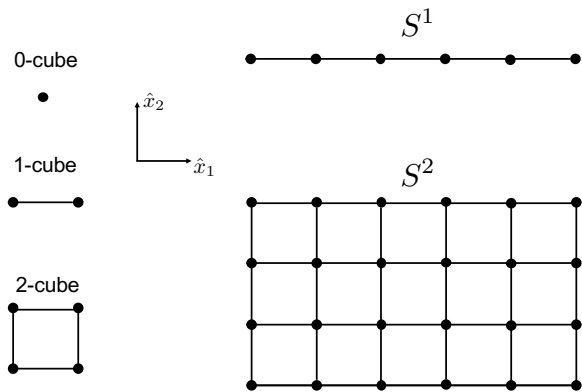


FIG. 3. Some examples of geometric objects n -cube and S^j embedded in D -dimensional hypercubic lattice.

$\langle \hat{x}_{i_1}, \hat{x}_{i_2}, \dots, \hat{x}_{i_{d_l}} \rangle$ to uniquely denote such a subspace. Among these d_l orthogonal directions, d_n ones come from the set $\mathcal{C}_{\gamma_{d_n}}^h$. As a result, the remaining $(d_l - d_n)$ ones are arbitrarily picked from the set $\mathcal{C}_{\gamma_{d_n}}^i$. Therefore, there are combinatorially $\binom{D-d_n}{d_l-d_n} \equiv \frac{(D-d_n)!}{(d_l-d_n)!(D-d_l)!}$ different choices of leaf space associated with the given γ_{d_n} .

It must be noted that, any lattice site inside the leaf space l has a coordinate with D components since the lattice site is in fact a point in D -dimensional lattice. Among D components, d_l components are free variables with orthogonal directions $\hat{x}_{i_1}, \hat{x}_{i_2}, \dots, \hat{x}_{i_{d_l}}$, which spans a d_l -dimensional subspace. The remaining $(D - d_l)$ coordinate components are fixed and simply equivalent to corresponding coordinate components of γ_{d_n} . Therefore, a leaf associated with a given γ_n can be uniquely labeled by l as long as γ_{d_n} is specified. For such a leaf l , we can define a set of orthogonal directions $\mathcal{L} = \{\hat{x}_{i_1}, \hat{x}_{i_2}, \dots, \hat{x}_{i_{d_l}}\}$, which will be used later.

Let us apply the above notation to the X-cube model (to be introduced in Sec. III B). The X-cube model has foliation structure [7, 22–25], where the leaf space dimension $d_l = 2$, and the model dimension $D = 3$. The direction index i in Eq. (5) can be also seen as an index for a leaf space l . For example, when $i = x$ and the vertex is $(0, 0, 0)$ (i.e., a 0-cube), $B_{(0,0,0)}^x$ corresponds to the

nearest four σ^z 's inside the $\langle \hat{y}, \hat{z} \rangle$ leaf (i.e., $\hat{y} - \hat{z}$ plane with $x = 0$). In this manner, for the Hamiltonian in the form of

$$H_{X-cube} = -J \sum_{\{\gamma_3\}} A_{\gamma_3} - K \sum_{\{\gamma_0\}} \sum_l B_{\gamma_0}^l \quad (1)$$

which is in fact the standard X-cube model that will be given in Eq. (5), there are in total $\binom{3-0}{2-0} = \binom{3}{2} = 3$ different leaf spaces: $\langle \hat{y}, \hat{z} \rangle$, $\langle \hat{x}, \hat{z} \rangle$, $\langle \hat{x}, \hat{y} \rangle$ planes associated with the vertex $(0, 0, 0)$. All of these planes pass through the vertex $(0, 0, 0)$.

Besides, as higher dimensional leaf spaces shall be used in the following sections, here it's also beneficial to give some examples of leaves in high dimensional models:

Example 1. — In the model-[1, 2, 3, 4] (to be studied in Sec. III C), the total space dimension $D = 4$ and the leaf space dimension $d_l = 3$. For a 1-cube $\gamma_1 = (0, 0, 0, \frac{1}{2})$, there are $\binom{4-1}{3-1} = 3$ leaves associated with it, which are respectively $\langle \hat{x}_1, \hat{x}_2, \hat{x}_4 \rangle$, $\langle \hat{x}_1, \hat{x}_3, \hat{x}_4 \rangle$ and $\langle \hat{x}_2, \hat{x}_3, \hat{x}_4 \rangle$. The coordinate component x_3 of each lattice site inside $\langle \hat{x}_1, \hat{x}_2, \hat{x}_4 \rangle$ is 0, which is exactly determined by x_3 of γ_1 .

Example 2. — In the model-[0, 1, 2, 4] (to be studied in Sec. IV C), the total space dimension $D = 4$ and the leaf space dimension $d_l = 2$. For a 0-cube $\gamma_0 = (0, 0, 0, 0)$, there are $\binom{4-0}{2-0} = 6$ leaves associated with it, which are respectively $\langle \hat{x}_1, \hat{x}_2 \rangle$, $\langle \hat{x}_1, \hat{x}_3 \rangle$, $\langle \hat{x}_1, \hat{x}_4 \rangle$, $\langle \hat{x}_2, \hat{x}_3 \rangle$, $\langle \hat{x}_2, \hat{x}_4 \rangle$ and $\langle \hat{x}_3, \hat{x}_4 \rangle$. Both coordinate components x_3 and x_4 of each lattice site inside $\langle \hat{x}_1, \hat{x}_2 \rangle$ are 0, which are exactly determined by x_3, x_4 of γ_0 .

Example 3. — In the model-[1, 2, 3, 5] (to be studied in Sec. IV C), the total space dimension $D = 5$ and the leaf space dimension $d_l = 3$. For a 2-cube $\gamma_2 = (0, 0, 0, \frac{1}{2}, \frac{1}{2})$, there are $\binom{5-2}{3-2} = 3$ leaves associated with it, which are respectively $\langle \hat{x}_1, \hat{x}_4, \hat{x}_5 \rangle$, $\langle \hat{x}_2, \hat{x}_4, \hat{x}_5 \rangle$ and $\langle \hat{x}_3, \hat{x}_4, \hat{x}_5 \rangle$. Both coordinate components x_2 and x_3 of each lattice site inside $\langle \hat{x}_1, \hat{x}_4, \hat{x}_5 \rangle$ are 0, which are exactly determined by x_2, x_3 of γ_2 .

Besides, as examples above suggest, the meaning of the 4 indexes in the 4-tuple notation of models are listed below:

- The first index d_n is the dimension of the d_n -cube where a B -term in the hamiltonian is defined on.

- The second index d_s is the dimension of the d_s -cube where a spin is defined on.
- The third index d_l is the dimension of the leaf spaces.
- The fourth index D is both the dimension of the D -cube where an A -term in the hamiltonian is defined on, and the dimension of the whole system.

A more detailed definition is given in Sec. IV.

C. Definition of “nearest” via L_1 -norm and L_1 -distance

L_1 -distance [86] is a distance function that is different from the Euclidean distance. In general, since there are various manners to define the length (a.k.a. norm) of a vector, and every well-defined length of the difference between two vectors can be used as a distance, we can use the L_1 -norm to give the so-called L_1 -distance. For vector $v = (x_1, x_2, \dots, x_d)$, its L_1 -norm is given by:

$$L_1(v) = |x_1| + |x_2| + \dots + |x_d|. \quad (2)$$

Then, by taking the L_1 -norm of the difference between two vectors as a distance function, we obtain the L_1 -distance between the two vectors. That is to say, for vector $v_1 = (x_1, x_2, \dots, x_d)$ and $v_2 = (y_1, y_2, \dots, y_d)$, their L_1 -distance is given by:

$$L_1(v_1, v_2) = |x_1 - y_1| + |x_2 - y_2| + \dots + |x_d - y_d|. \quad (3)$$

In this article, we use L_1 distance to define whether two objects are “nearest”. If an m -cube and an n -cube are said to be “nearest” to each other, the L_1 distance should be: $L_1(\gamma_m, \gamma_n) = \frac{|m-n|}{2}$ when $m \neq n$. For $m = n$, we specially define two n -cubes being nearest if $L_1(\gamma_n^1, \gamma_n^2) = 1$.

D. Stacking of cubes: straight string, flat membrane, and beyond

Moreover, in order to specify a region in hypercubic lattice, we also need a group of notations to denote “flat” objects composed by n -cubes, like higher dimensional analogs of straight strings and flat membranes. Here, we define a j -dimensional analog of a straight string (in the original lattice) S^j as a stack of nearest j -cubes where all the j -cubes share the same coordinates along orthogonal directions collected in the set $\mathcal{C}_{\gamma_j}^i$. The simplest examples are straight lines S^1 and flat membranes S^2 as shown in Fig. 3. In this figure, let us assume $D = 3$. Then, $\mathcal{C}_{\gamma_1}^i = \{\hat{x}_2, \hat{x}_3\}$, $\mathcal{C}_{\gamma_2}^i = \{\hat{x}_3\}$. All 1-cubes (i.e., links) in S^1 share same integer-valued coordinates along both \hat{x}_2 and \hat{x}_3 , and all 2-cubes (i.e., plaquettes) in S^2 share same integer-valued coordinates along \hat{x}_3 . When we need to

specify a S^{i-1} which is located at the convergence of two S^i , we will also use C^{i-1} to refer to it.

In a similar manner, we may define flat geometric objects in the dual lattice of the original lattice. More concretely, a k -dimensional analog (denoted by D^k) of a flat membrane in the dual lattice can be defined as a stack of nearest $(D-k)$ -cubes in the original lattice, where all the $(D-k)$ -cubes share the same values for coordinates along orthogonal directions collected in the set $\mathcal{C}_{\gamma_{D-k}}^h$. Alternatively speaking, a D^k is just an S^k if the dual lattice and original lattice are switched. For instance, a D^2 in 3D space is a connected set of parallel links (i.e., 1-cubes γ_1) all of which share the same $\mathcal{C}_{\gamma_1}^h$. The creation operator of fractons in the X-cube model is defined on a D^2 in 3D.

Specially, sometimes we may also use D_p^k to denote a stack of nearest p -cubes in the original lattice, where all the p -cubes share the same values for coordinates along orthogonal directions collected in the set $\mathcal{C}_{\gamma_p}^h \cup \mathcal{C}_{\gamma_p}^{si}$. Here $\mathcal{C}_{\gamma_p}^{si}$ is a subset of $\mathcal{C}_{\gamma_p}^i$ which satisfies $|\mathcal{C}_{\gamma_p}^{si}| = D - k - p$. Different from the previously defined objects, since $\mathcal{C}_{\gamma_p}^{si}$ is not completely specified, a D_p^k can't be totally determined by γ_p , k and p , so additional information is needed to specify a D_p^k . For example, in 3D X-cube model we will use D_1^1 , i.e., $p = k = 1$ and $D = 3$. Let us consider a 1-cube $\gamma_1 = (\frac{1}{2}, 0, 0)$, so the two sets of orthogonal directions are fixed: $\mathcal{C}_{\gamma_1}^h = \{\hat{x}_1\}$ and $\mathcal{C}_{\gamma_1}^i = \{\hat{x}_2, \hat{x}_3\}$. Therefore, $\mathcal{C}_{\gamma_1}^{si} = \{\hat{x}_2\}$ or $\{\hat{x}_3\}$, leading to two choices: $\mathcal{C}_{\gamma_1}^h \cup \mathcal{C}_{\gamma_1}^{si} = \{\hat{x}_1, \hat{x}_2\}$ or $\{\hat{x}_1, \hat{x}_3\}$. As a result, there are two possible directions for stacking 1-cubes in D_1^1 , i.e., $\{(\frac{1}{2}, 0, j) | j = 0, 1, 2, \dots\}$ and $\{(\frac{1}{2}, i, 0) | i = 0, 1, 2, \dots\}$. When we need to specify a D_p^k in the remainder of this article, additional information will always be given in the context.

As for boundaries, the boundary ∂S^1 is simply given by the two endpoints of S^1 ; the boundary ∂S^2 is a closed string; It's a bit difficult to define the boundary of a D^k , but the vertices of D^k can be naturally obtained by regarding D^k as a k -dimensional polytope.

III. $[D-3, D-2, D-1, D]$ MODEL SERIES

A. Construction of $[D-3, D-2, D-1, D]$ models

In this section, we first consider models on a D -dimensional hypercubic lattice where spins are located on $(D-2)$ -cubes instead of links, while keeping the basic form of X-cube Hamiltonian unaltered. By introducing a 4-tuple notation, this consideration is called $[D-3, D-2, D-1, D]$ models. The Hamiltonian of general form is given by ($J > 0$ and $K > 0$ are always assumed):

$$H_D = -J \sum_{\{\gamma_D\}} A_{\gamma_D} - K \sum_{\{\gamma_{D-3}\}} \sum_l B_{\gamma_{D-3}}^l, \quad (4)$$

where A_{γ_D} is the product of spin operators σ^x 's located on the centers of $(D-2)$ cubes that are nearest⁵ to hypercube γ_D . In this series of models, a B operator is associated with a d_n -cube and a leaf space l with $d_n = D-3$ and $d_l = D-1$. More concretely, $B_{\gamma_{D-3}}^l$ is the product of all σ^z 's which are not only nearest to γ_{D-3} but also located inside the leaf l . The number of leaf spaces associated with each γ_{d_n} is always $\binom{D-d_n}{d_l-d_n} \equiv \frac{(D-d_n)!}{(d_l-d_n)!(D-d_l)!} = \frac{3!}{2!} = 3$ regardless of D . In the following subsections, we will concentrate on $[0, 1, 2, 3]$ and $[1, 2, 3, 4]$ these two models to explore their excitation spectra. Especially there are simple dimension reduction rules for simple excitations in this model series as shown in Fig. 1. The details are collected in Table II.

TABLE II. Typical examples of simple excitations (i.e., \mathbf{E}^s sector) in $[D-3, D-2, D-1, D]$ models.

D	Excitations labels	Creation operators
3	(0, 0)	$\prod_{\gamma_1 \in D^2} \sigma_{\gamma_1}^z$
	(0, 1)	$\prod_{\gamma_1 \in S^1} \sigma_{\gamma_1}^x$
	(0, 2)	$\prod_{\gamma_1 \in D_1^1} \sigma_{\gamma_1}^z$
4	(0, 0)	$\prod_{\gamma_2 \in D^2} \sigma_{\gamma_2}^z$
	(1, 2)	$\prod_{\gamma_2 \in S^2} \sigma_{\gamma_2}^x$
	(0, 3)	$\prod_{\gamma_2 \in D_2^1} \sigma_{\gamma_2}^z$
5	(0, 0)	$\prod_{\gamma_3 \in D^2} \sigma_{\gamma_3}^z$
	(2, 3)	$\prod_{\gamma_3 \in S^3} \sigma_{\gamma_3}^x$
	(0, 4)	$\prod_{\gamma_3 \in D_3^1} \sigma_{\gamma_3}^z$

B. The X-cube model as $[0, 1, 2, 3]$

The well-understood X-cube model is labeled by $[0, 1, 2, 3]$ in our notation. As the name suggests, X-cube model is defined on a cubic lattice, with $1/2$ -spins sitting on links. The Hamiltonian is of the form [8]:

$$H_{X\text{-cube}} = -J \sum_c A_c - K \sum_v \sum_i B_v^i \quad (5)$$

which is alternatively written as Eq. (1) in terms of geometric notations. Here, the term A_c of a given cube c consists of the product of the x components (i.e., σ_x) of the twelve spins around the cube c ; B_v^i means the product of σ_z 's that are (i) inside the 2D plane that is perpendicular to the direction i and (ii) nearest to the vertex v . The summation of c and v are respectively over all

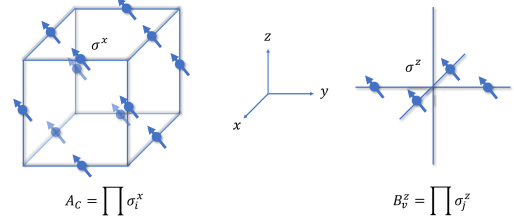


FIG. 4. Terms in the X-cube Hamiltonian. As shown in the figure, the A_c term is composed of the 12 spins (σ^x) on the edges of the cube, while the B_v^z term is composed of the 4 spins (σ^z) on the legs of a vertex. For simplicity, only one of the 3 B_v^i terms ($i = x, y, z$) on the vertex v is shown, while $B_v^x = \prod \sigma^z$ and $B_v^y = \prod \sigma^z$ are not shown.

cubes and vertices, while the summation of i is over the three spatial dimensions. The model is shown pictorially in Fig. 4.

With the σ^z basis, we can regard the links with $\sigma^z = -1$ as being “occupied” by strings and the links with $\sigma^z = 1$ spins as being “unoccupied”. In this manner, the total Hilbert space can be alternatively represented by all kinds of different string configurations including both open and closed strings. Then, by solving the equations $A_c = 1, \forall c$ and $B_v^i = 1, \forall v$, with the open boundary condition, we can directly derive the ground state as $|s_i\rangle: |\Phi\rangle = \prod_c \frac{1+A_c}{\sqrt{2}} |\uparrow\uparrow\uparrow \dots \uparrow\rangle$, where $|\uparrow\uparrow\uparrow \dots \uparrow\rangle$ refers to the state with zero string. In the remainder of this article, $|\uparrow\uparrow\uparrow \dots \uparrow\rangle$ will be used as a reference state frequently. The ground state of Eq. (5) is dubbed as “cage-net” condensation [25]. If we consider the X-cube model on a 3-torus of the size $L \times L \times L$, the ground state will be degenerate, and the ground state degeneracy (GSD) is given by $\log_2 \text{GSD} = 6L - 3$. The linear term here is also a significant feature of fracton orders, as it means that the GSD grows subextensively [7, 8].

Some representative excitations of the X-cube model are summarized in Table III. In the X-cube model, there are two most important classes of excitations—lineons and fractons, which are respectively originated from the eigenvalue flip of B_v^i and A_c terms. Let us explain in details:

- *An excited state with one lineon.* The $B_v^i = -1$ excitations, dubbed “lineons”, are generated by string operator $W(S^1) = \prod_{\gamma_1 \in S^1} \sigma_{\gamma_1}^x$ composed of $\sigma_{\gamma_1}^x$ along the open string S^1 which must be absolutely straight. The point-like excitations at the endpoints of a string are restricted in the line where the string sits, thus the name “lineons”. In our notation, the end-of-string excitations are (0, 1)-type point-like excitations and belong to \mathbf{E}^s . For example, if the string S^1 is along \hat{x} -axis, the eigenvalues of both B_v^y and B_v^z at each endpoint of S^1 will be flipped, rendering $2K$ energy cost. Therefore, there are in total three “lineons”, denoted by ℓ_x, ℓ_y , and ℓ_z , where the subscripts denote the directions of

⁵ The accurate definition of “nearest” is given in Sec. II C

TABLE III. Typical examples of excitations in $[0, 1, 2, 3]$ model. Simple excitations are labeled by a pair of integers.

Excitations	Sectors	Flipped stabilizers	Creation operators
fracton: $(0, 0)$	E^s	A_{γ_3}	$\prod_{\gamma_1 \in D^2} \sigma_{\gamma_1}^z$
lineon: $(0, 1)$	E^s	$B_{\gamma_0}^l$	$\prod_{\gamma_1 \in S^1} \sigma_{\gamma_1}^x$
connected planeon: $(0, 2)$	E^s	A_{γ_3}	$\prod_{\gamma_1 \in D_1^1} \sigma_{\gamma_1}^z$
disconnected planeon	E^d	A_{γ_3}	$\prod_{\gamma_1 \in D^2} \sigma_{\gamma_1}^z$

straight lines along which lineons can move.

- *An excited state with two spatially separate lineons.* If ℓ_x and ℓ_y are able to meet at some point, they fuse into ℓ_z which is still a point, a zero-dimensional manifold. An excited state with *these* two spatially separate point-like pieces (i.e., ℓ_x and ℓ_y) belongs to \tilde{E}^d which is, by definitions in Sec. IB, eventually E^s . But ℓ_x and ℓ_y are unable to meet each other if the two straight lines do not intersect. If this is the case, the geometric shape of the excited state with a pair of ℓ_x and ℓ_y is intrinsically disconnected. As a result, such an excited state belongs to E^d rather than \tilde{E}^d . Likewise, if there are two ℓ_x lineons which move along two parallel straight lines of x direction, such an excited state is also in E^d since the geometric shape (two spatially separate points) are intrinsically disconnected.
- *An excited state with one fracton.* In addition to lineons, the $A_c = A_{\gamma_3} = -1$ excitations correspond to fractons (i.e. $(0, 0)$ -type excitations) associated to the cube c . Fractons, as point-like excitations, belong to E^s . More precisely, fractons are created by operators of the form $W(D^2) = \prod_{\gamma_1 \in D^2} \sigma_{\gamma_1}^z$, where D^2 is an absolutely flat 2-dimensional membrane in the dual lattice. The cubes c 's are located at the corners of D^2 , each of which requires J energy cost. For example, if D^2 is simply a rectangular, there will be four emerged fractons at the four corners. One can show that fractons are totally immobile. More concretely, moving a single fracton by applying spin operators will create additional new fractons nearby.
- *An excited state with two fractons.* Despite that fractons are immobile, a pair of two nearby fractons generated by one membrane can move freely in the 2D plane perpendicular to the link between the two combined fractons. Thus these pairs, dubbed “connected planeons”, are identified as $(0, 2)$ -type excitations in E^s sector in our notation when the component fractons are exactly next to each other. If the two component fractons are separate, the corresponding excitation is called “disconnected planeons” which belong to E^d . Two types of planeons cannot be changed to each other by local opera-

tors since they belong to different sectors of Hilbert space.

C. Simple excitations in the model-[1, 2, 3, 4]

In the remainder of this section, we focus on the model-[1, 2, 3, 4]. In this model, for a specific 4-cube $\gamma_4 = (\frac{1}{2}, \frac{1}{2}, \frac{1}{2}, \frac{1}{2})$ and a specific 1-cube $\gamma_1 = (0, 0, 0, \frac{1}{2})$ respectively, we have⁶

$$\begin{aligned}
A_{(\frac{1}{2}, \frac{1}{2}, \frac{1}{2}, \frac{1}{2})} &= \sigma_{(0,0,\frac{1}{2},\frac{1}{2})}^x \sigma_{(0,1,\frac{1}{2},\frac{1}{2})}^x \sigma_{(1,0,\frac{1}{2},\frac{1}{2})}^x \sigma_{(1,1,\frac{1}{2},\frac{1}{2})}^x \\
&\sigma_{(0,\frac{1}{2},0,\frac{1}{2})}^x \sigma_{(0,\frac{1}{2},1,\frac{1}{2})}^x \sigma_{(1,\frac{1}{2},0,\frac{1}{2})}^x \sigma_{(1,\frac{1}{2},1,\frac{1}{2})}^x \\
&\sigma_{(0,\frac{1}{2},\frac{1}{2},0)}^x \sigma_{(0,\frac{1}{2},\frac{1}{2},1)}^x \sigma_{(1,\frac{1}{2},\frac{1}{2},0)}^x \sigma_{(1,\frac{1}{2},\frac{1}{2},1)}^x \\
&\sigma_{(\frac{1}{2},0,0,\frac{1}{2})}^x \sigma_{(\frac{1}{2},0,1,\frac{1}{2})}^x \sigma_{(\frac{1}{2},1,0,\frac{1}{2})}^x \sigma_{(\frac{1}{2},1,1,\frac{1}{2})}^x \\
&\sigma_{(\frac{1}{2},0,\frac{1}{2},0)}^x \sigma_{(\frac{1}{2},0,\frac{1}{2},1)}^x \sigma_{(\frac{1}{2},1,\frac{1}{2},0)}^x \sigma_{(\frac{1}{2},1,\frac{1}{2},1)}^x \\
&\sigma_{(\frac{1}{2},\frac{1}{2},0,0)}^x \sigma_{(\frac{1}{2},\frac{1}{2},0,1)}^x \sigma_{(\frac{1}{2},\frac{1}{2},1,0)}^x \sigma_{(\frac{1}{2},\frac{1}{2},1,1)}^x,
\end{aligned} \tag{6}$$

and

$$\begin{aligned}
B_{(0,0,0,\frac{1}{2})}^{(\hat{x}_1, \hat{x}_2, \hat{x}_4)} &= \sigma_{(\frac{1}{2},0,0,\frac{1}{2})}^z \sigma_{(-\frac{1}{2},0,0,\frac{1}{2})}^z \sigma_{(0,\frac{1}{2},0,\frac{1}{2})}^z \sigma_{(0,-\frac{1}{2},0,\frac{1}{2})}^z, \\
B_{(0,0,0,\frac{1}{2})}^{(\hat{x}_2, \hat{x}_3, \hat{x}_4)} &= \sigma_{(0,\frac{1}{2},0,\frac{1}{2})}^z \sigma_{(0,-\frac{1}{2},0,\frac{1}{2})}^z \sigma_{(0,0,\frac{1}{2},\frac{1}{2})}^z \sigma_{(0,0,-\frac{1}{2},\frac{1}{2})}^z, \\
B_{(0,0,0,\frac{1}{2})}^{(\hat{x}_1, \hat{x}_3, \hat{x}_4)} &= \sigma_{(\frac{1}{2},0,0,\frac{1}{2})}^z \sigma_{(-\frac{1}{2},0,0,\frac{1}{2})}^z \sigma_{(0,0,\frac{1}{2},\frac{1}{2})}^z \sigma_{(0,0,-\frac{1}{2},\frac{1}{2})}^z.
\end{aligned} \tag{7}$$

Although the model looks strange at first sight, it is just a generalization of the 3D X-cube model given by Eq. (5) and its equivalent form Eq. (1) (another 4D generalization is the the model-[0, 1, 2, 4], which is discussed in Sec. IV C). As we can see that once we choose $D = 3$ in Eq. (4), the model would simply reduce to Eq. (1). In other words, the X-cube model is the simplest case in the series $[D - 3, D - 2, D - 1, D]$. Furthermore, an A_{γ_D} always overlaps with a nearest B operator by even number of spins, as an A_{γ_D} always covers one of each pair of spins linked by a nearest γ_{D-3} , and a B operator is composed of 2 such pairs. Therefore, our generalized

⁶ See the “Example 1” in Sec. IIB for an introduction to the leaves in model-[1, 2, 3, 4].

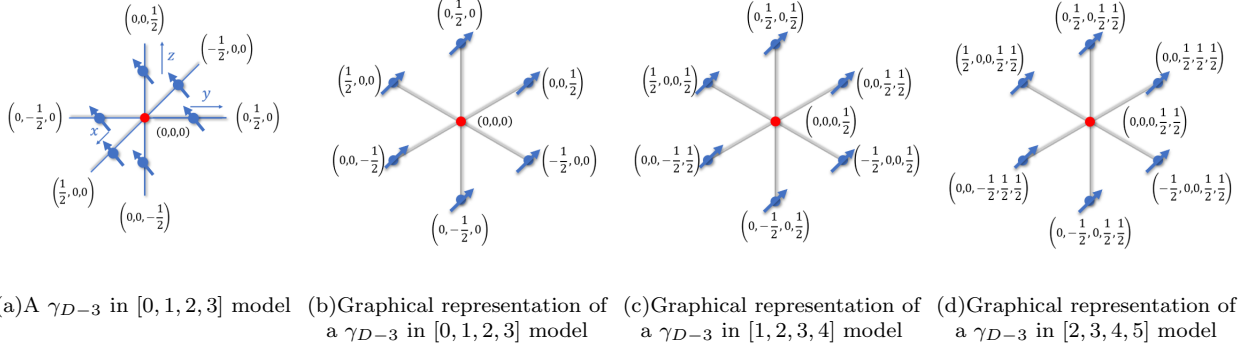


FIG. 5. Graphical representation of γ_{D-3} in some $[D-3, D-2, D-1, D]$ models. Here, (b) is the graph representation of the $\gamma_{D-3} = (0, 0, 0)$ presented in (a). As we can see, in higher dimensions, the graph representation of a γ_{D-3} is completely the same as in the 3D case: a γ_{D-3} always connects 3 pairs of γ_{D-2} , which means 3 pairs of spins in $[D-3, D-2, D-1, D]$ models.

models are still exactly solvable. Fig. 5 gives a graph demonstration.

The ground state configuration must satisfy the following conditions: $A_{\gamma_D}|\phi\rangle = |\phi\rangle$, $B_{\gamma_{D-3}}^l|\phi\rangle = |\phi\rangle$, $\forall \gamma_D, \gamma_{D-3}, l$. Topological excitations appear in the region where one or a proper combination of these conditions is violated. In the σ^z basis, we can regard the ground states as condensations of “ D -cage nets”, where “ D -cage” is the D -dimensional analog of the “cage” proposed in Ref. [25]. When the boundary of the system is open, we can obtain the ground state wave function as the equal-weight superposition of all D -cages: $|\Phi\rangle = \prod_{\gamma_D} \frac{1+A_{\gamma_D}}{\sqrt{2}} |\uparrow\uparrow\uparrow \dots \uparrow\rangle$. Here $|\uparrow\uparrow\uparrow \dots \uparrow\rangle$ is a reference state where spins are all upward along z -axis.

Next, we move on to the excitation spectrum of the model Hamiltonian given by Eq. (4). We shall begin with the energy cost of “simple excitations”. When the lattice constant a goes to 0, these excitations will look like some connected manifolds, like points, strings, membranes and so on. Elementary introductions to manifold can be found on Page 219 of Ref. [85].

Analogous to the original X-cube model, the most representative simple excitations in the model- $[1, 2, 3, 4]$ can be classified into two classes: $(0, 0)$ -type excitations and $(1, 2)$ -type excitations. The former are excited by operators $W(D^2) = \prod_{\gamma_2 \in D^2} \sigma_{\gamma_2}^z$, resulting in eigenvalue flip (i.e., $1 \rightarrow -1$) of A_{γ_4} for γ_4 's at the corners of the D^2 . The latter are excited by $W(S^2) = \prod_{\gamma_2 \in S^2} \sigma_{\gamma_2}^x$, resulting in eigenvalue flip (i.e., $1 \rightarrow -1$) of $B_{\gamma_1}^l$ for γ_1 's along ∂S^2 . For the sake of convenience, we will use the expressions $A = -1$ and $B = -1$ to describe such eigenvalue flip. The general definition of the notations D^2 and S^2 can be found in Sec. II. Starting from the next subsection, we will discuss the excitation spectrum of this model systematically. Some excitations are collected in Table IV.

1. $(0, 0)$ -type point-like excitations (fractons)

Firstly, let's consider the $(0, 0)$ -type excitations, i.e., fractons. When we act $W(D^2) = \prod_{\gamma_2 \in D^2} \sigma_{\gamma_2}^z$ on the ground state, the minimal polytope P that envelops all the spins (σ^z 's) acted on by $W(D^2)$ is 4-dimensional. Obviously, all 4-cube operators A_{γ_4} inside P will contain even number of σ^x 's that are acted on by $W(D^2)$, which keeps eigenvalues of all such operators A_{γ_4} unaltered, i.e., $A_{\gamma_4} = 1$ for $\gamma_4 \in P$. Nevertheless, for all γ_4 's that sit on the corners (i.e., vertices of D^2) have only one spin per γ_4 that is acted on by $W(D^2)$, which flips the eigenvalue of these A_{γ_4} , i.e., $A_{\gamma_4} = -1$ for such γ_4 's.

For example, we can apply $W(D^2) = \prod_{\gamma_1 \in D^2} \sigma_{\gamma_1}^z$ on the ground state, where, according to the definition in Sec. II, $D^2 = \{(i, j, \frac{1}{2}, \frac{1}{2}) | i, j = 0, 1, \dots, L\}$. Geometrically, D^2 forms a square of $L \times L$, $L \in \mathbb{Z}$. For any hypercube $(m + \frac{1}{2}, n + \frac{1}{2}, \frac{1}{2}, \frac{1}{2})$, where $m, n = 0, 1, 2, \dots, L-1$, there are always four spins located at respectively $(m, n, \frac{1}{2}, \frac{1}{2})$, $(m+1, n, \frac{1}{2}, \frac{1}{2})$, $(m, n+1, \frac{1}{2}, \frac{1}{2})$ and $(m+1, n+1, \frac{1}{2}, \frac{1}{2})$ that are acted on by $W(D^2)$. Therefore, the associated operators A_{γ_4} have their eigenvalues unchanged, i.e., $A_{\gamma_4} = 1$. Only for the 4-cubes at the corners, like $\gamma_4 = (-\frac{1}{2}, -\frac{1}{2}, \frac{1}{2}, \frac{1}{2})$, there is just one spin per γ_4 acted on by $W(D^2)$, thus $A_{\gamma_4} = -1$ (i.e., we can say the operator is excited). As a result, it's straightforward to conclude that these excitations are of $(0, 0)$ -type, as any movement of such an excitation will create more corners associated with additional excitations and energy cost. See Fig. 6(a) for a schematic demonstration.

2. $(0, 3)$ -type point-like excitations (connected volumeons)

In the model $[1, 2, 3, 4]$, a pair of two fractons at two neighbouring corners of a membrane in the dual lattice are not a anyon anymore. Instead, these pairs become

TABLE IV. Typical examples of excitations in the model-[1, 2, 3, 4]. Note: excitations in Sec. III E are collected separately in Table V.

Excitations	Sectors	Flipped stabilizers	Creation operators
fracton: (0, 0)	E^s	A_{γ_4}	$\prod_{\gamma_2 \in D^2} \sigma_{\gamma_2}^z$
(1, 2)	E^s	$B_{\gamma_1}^l$	$\prod_{\gamma_2 \in S^2} \sigma_{\gamma_2}^x$
connected volumeon: (0, 3)	E^s	A_{γ_4}	$\prod_{\gamma_2 \in D_{\frac{1}{2}}^1} \sigma_{\gamma_2}^z$
chairon	E^c	$B_{\gamma_1}^l$	$\prod_{\gamma_2 \in S_I^2} \sigma_{\gamma_2}^x \prod_{\gamma_2 \in S_{II}^2} \sigma_{\gamma_2}^x$, where $\partial S_I^2 \cap \partial S_{II}^2 = C^1 \neq \emptyset$
yuon	E^c	$B_{\gamma_1}^l$	$\prod_{\gamma_2 \in S_I^2} \sigma_{\gamma_2}^x \prod_{\gamma_2 \in S_{II}^2} \sigma_{\gamma_2}^x \prod_{\gamma_2 \in S_{III}^2} \sigma_{\gamma_2}^x$, where $\partial S_I^2 \cap \partial S_{II}^2 \cap \partial S_{III}^2 = C^1 \neq \emptyset$
disconnected volumeon	E^d	A_{γ_4}	$\prod_{\gamma_2 \in D^2} \sigma_{\gamma_2}^z$

“volumeons” for an observer in a 4D world. While it should be noticed that such a pair in general can belong to either E^s sector or E^d sector, and here we only consider the E^s -type pair in which two γ_4 associated with the two fractons are nearest to each other, so we can label it by (0, 3). This excited state is called “connected volumeons”, analogous to “connected planeons” in Table III. For instance, we can consider acting the open string operator $W(D_{\frac{1}{2}}^1) = \prod_{\gamma_2 \in D_{\frac{1}{2}}^1} \sigma_{\gamma_2}^z$ on the ground state, where $D_{\frac{1}{2}}^1 = \{(0, i, \frac{1}{2}, \frac{1}{2}) | i = 0, 1, 2, 3, \dots, L-1, L\}$.⁷ After that, in the neighborhood of an endpoint of the $D_{\frac{1}{2}}^1$, e.g., $(0, 0, \frac{1}{2}, \frac{1}{2})$, there are two nearest 4-cube operators A_{γ_4} with $\gamma_4 = (-\frac{1}{2}, -\frac{1}{2}, \frac{1}{2}, \frac{1}{2})$ and $\gamma_4 = (\frac{1}{2}, -\frac{1}{2}, \frac{1}{2}, \frac{1}{2})$ whose eigenvalues are flipped. These two 4-cubes form a pair of nearest fractons, whose energy is $2J$. Define a vector \mathbf{r} connecting the two 4-cubes: $\mathbf{r} = (\frac{1}{2} - (-\frac{1}{2}), -\frac{1}{2} - (\frac{1}{2}), \frac{1}{2} - \frac{1}{2}, \frac{1}{2} - \frac{1}{2}) = (1, 0, 0, 0)$. Then, the pair of fractons can be regarded as a dipole whose moment point in the direction \mathbf{r} , i.e., \hat{x}_1 .

For the issue of mobility, let us attempt to act $\sigma_{(0, -\frac{1}{2}, 0, \frac{1}{2})}^z$ to move the pair out of the line where the string is located at. As we can see, since $\sigma_{(0, -\frac{1}{2}, 0, \frac{1}{2})}^z$ flips the sign of A_{γ_4} for $\gamma_4 \in \{(\frac{1}{2}, -\frac{1}{2}, \frac{1}{2}, \frac{1}{2}), (-\frac{1}{2}, -\frac{1}{2}, -\frac{1}{2}, \frac{1}{2}), (\frac{1}{2}, -\frac{1}{2}, -\frac{1}{2}, \frac{1}{2}), (-\frac{1}{2}, -\frac{1}{2}, \frac{1}{2}, \frac{1}{2})\}$, $\sigma_{(0, -\frac{1}{2}, 0, \frac{1}{2})}^z$ can move the pair along \hat{x}_4 direction. Since $(0, -\frac{1}{2}, 0, \frac{1}{2})$ and $(0, -\frac{1}{2}, \frac{1}{2}, 0)$ are symmetric about the string, the pair can also be moved along the \hat{x}_3 direction. As a result, the mobility of the pair is restricted in the 3-dimensional leaf space $\langle \hat{x}_2, \hat{x}_3, \hat{x}_4 \rangle$ with $x_1 = 0$.

3. (1, 2)-type string excitations of 6 flavors

Next we consider excitations associated with flipped eigenvalues of $B_{\gamma_1}^l$. For each γ_1 , there are three associated leaves labeled by l . We find that there are 6 flavors of (1, 2)-type excitations— string excitations⁸ that are created and moved within a certain plane *only*, i.e., \hat{x}_1 - \hat{x}_2 , \hat{x}_1 - \hat{x}_3 , \hat{x}_1 - \hat{x}_4 , \hat{x}_2 - \hat{x}_3 , \hat{x}_2 - \hat{x}_4 , and \hat{x}_3 - \hat{x}_4 . An example is given in Fig. 6(b) (see also Fig. 7(a)). We use the symbol “(1, 2) $^{\hat{x}_i, \hat{x}_j}$ ” with two integers $1 \leq i < j \leq 4$ to specify flavors.

More concretely, let us apply an open membrane operator $W(S^2) = \prod_{\gamma_2 \in S^2} \sigma_{\gamma_2}^x$ on the ground state. For γ_1 's at the interior of S^2 , by noting that there always exists exactly one pair of spins linked by each γ_1 being acted on by $W(S^2)$, the associated operators $B_{\gamma_1}^l$ will keep their eigenvalues (i.e., $B = 1$) unaltered after $W(S^2)$ is applied. Only for $\gamma_1 \in \partial S^2$, i.e., γ_1 's that form the boundary of S^2 , the eigenvalues of the associated operators $B_{\gamma_1}^l$ will be flipped, i.e., $B = -1$, as shown in Fig. 6(b). That is to say, these $B_{\gamma_1}^l$ operators with flipped eigenvalues constitute string excitations, of which the energy cost (i.e., excitation energy) is proportional to the length of the string.

Analogous to X-cube model, $W(S^2)$ here can be classified into 6 “flavors” according to 6 different planes (i.e., \hat{x}_1 - \hat{x}_2 , \hat{x}_1 - \hat{x}_3 , \hat{x}_1 - \hat{x}_4 , \hat{x}_2 - \hat{x}_3 , \hat{x}_2 - \hat{x}_4 , and \hat{x}_3 - \hat{x}_4) where S^2 is located, and $W(S^2)$ of different flavors will flip different combinations of $B_{\gamma_1}^l$'s. In general, after applying $W(S^2)$ with S^2 being inside the \hat{x}_i - \hat{x}_j plane, there will be exactly two flipped $B_{\gamma_1}^l$ terms at each γ_1 along ∂S^2 , i.e., $B_{\gamma_1}^{\langle \hat{x}_i, \hat{x}_j, \hat{x}_k \rangle}$ and $B_{\gamma_1}^{\langle \hat{x}_i, \hat{x}_j, \hat{x}_h \rangle}$. Here $i, j, k, h \in \{1, 2, 3, 4\}$ and i, j, k, h are all different from each other. For example, by acting $W(S^2)$ on the ground state, where

⁷ Here “string” means that all spins acted on by the operator form an open string. The precise definition of $D_{\frac{1}{2}}^1$ is given in Sec. II).

⁸ Both words “string” and “loop” will be used for the name of such excitations.

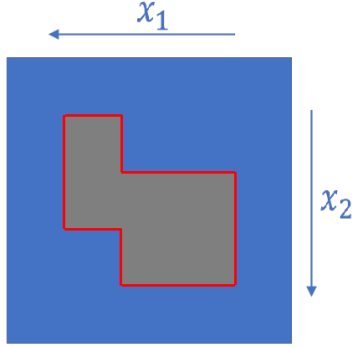
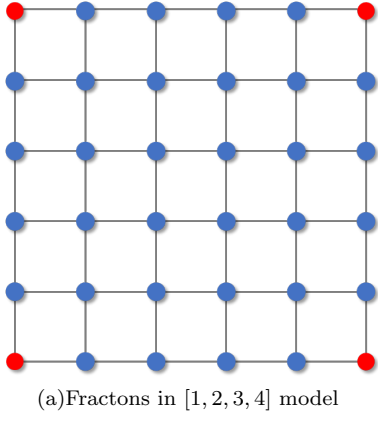


FIG. 6. Fractons and string excitations in the model [1, 2, 3, 4]. (a) demonstrates the distribution of fractons excited by $W(D^2) = \prod_{\gamma_2 \in D^2} \sigma_{\gamma_2}^z$. Flipped spins sitting on 2-cubes represented by dots are distributed on the sites of a 2-dimensional array, which is exactly the D^2 . The red dots at the corners of the D^2 refer to the spins that are nearest to an excited nearest 4-cube operator A_{γ_d} , and the blue dots refer to the spins whose nearest A_{γ_d} 's are not excited at all. In (b) the blue plaquettes label untouched spins while the grey plaquettes label the spins on which $W(D^2)$ acts. The string excitation as the domain wall is highlighted with red lines.

$S^2 = \{(n + \frac{1}{2}, m + \frac{1}{2}, 0, 0) | m, n = 0, 1, 2, \dots, L - 1\}$, for an arbitrary γ_1 along the boundary of S^2 , the eigenvalues of both $B_{\gamma_1}^{(\hat{x}_1, \hat{x}_2, \hat{x}_3)}$ and $B_{\gamma_1}^{(\hat{x}_1, \hat{x}_2, \hat{x}_4)}$ will be flipped. As a result, we find that the energy cost of this string excitation labeled by $(1, 2)^{\hat{x}_1, \hat{x}_2}$ in the model-[1, 2, 3, 4] is $2KL$, where L is the length of the string. Before moving forward, let us summarize the ‘‘stabilizers’’ whose eigenvalues are flipped for (1, 2)-type excitations of each flavor ($\gamma_1 \in \partial S^2$):

- $(1, 2)^{\hat{x}_1, \hat{x}_2}$: $B_{\gamma_1}^{(\hat{x}_1, \hat{x}_2, \hat{x}_3)}$ and $B_{\gamma_1}^{(\hat{x}_1, \hat{x}_2, \hat{x}_4)}$ (note: an example is given in Fig. 7(a).)
- $(1, 2)^{\hat{x}_1, \hat{x}_3}$: $B_{\gamma_1}^{(\hat{x}_1, \hat{x}_2, \hat{x}_3)}$ and $B_{\gamma_1}^{(\hat{x}_1, \hat{x}_3, \hat{x}_4)}$

- $(1, 2)^{\hat{x}_1, \hat{x}_4}$: $B_{\gamma_1}^{(\hat{x}_1, \hat{x}_2, \hat{x}_4)}$ and $B_{\gamma_1}^{(\hat{x}_1, \hat{x}_3, \hat{x}_4)}$
- $(1, 2)^{\hat{x}_2, \hat{x}_3}$: $B_{\gamma_1}^{(\hat{x}_1, \hat{x}_2, \hat{x}_3)}$ and $B_{\gamma_1}^{(\hat{x}_2, \hat{x}_3, \hat{x}_4)}$
- $(1, 2)^{\hat{x}_2, \hat{x}_4}$: $B_{\gamma_1}^{(\hat{x}_1, \hat{x}_2, \hat{x}_4)}$ and $B_{\gamma_1}^{(\hat{x}_2, \hat{x}_3, \hat{x}_4)}$
- $(1, 2)^{\hat{x}_3, \hat{x}_4}$: $B_{\gamma_1}^{(\hat{x}_1, \hat{x}_3, \hat{x}_4)}$ and $B_{\gamma_1}^{(\hat{x}_2, \hat{x}_3, \hat{x}_4)}$

For the issue of mobility and deformability, the string excitation has a novel property here: it is restricted in the 2D plane where S^2 lies. Without loss of generality, as shown in Fig. 7, let us try to move the string excitation out of the plane where S^2 lies, by folding S^2 in $\hat{x}_1 - \hat{x}_2$ plane into S_I^2 in $\hat{x}_1 - \hat{x}_3$ plane and S_{II}^2 in $\hat{x}_1 - \hat{x}_2$ plane. The crease line denoted by C^1 is along \hat{x}_1 direction. Nevertheless, this process will cost additional energy localized along C^1 . Therefore, moving or deforming the (1, 2)-type excitation out of the original plane is forbidden. Alternatively speaking, folding the loop in (a) only results in the state in (b) which is not a single loop state, thus deformation out of plane is forbidden. So, what does free deformation look like? In a pure topological order, a loop in (a) can be sent to (c) by local operators such that the loop gradually evolves into $\hat{x}_1 - \hat{x}_2$ plane without any obstruction. In Sec. III D, we will see that the excited state represented by Fig. 7(b) actually belongs to E^c sector.

But can the string excitation move and deform freely within the plane where it is located? It is easy to see that by applying $W(S^2)$ one can change the geometric shape of the string within the same plane. Moreover, no additional energy cost is required as long as the total length L is unchanged. In this sense, the string excitation can move and deform freely within a 2D subspace, so that such string excitations in our notation are labeled by (1, 2). For instance, let us apply

$$W(S_I^2) = \prod_{\gamma_2 \in S_I^2} \sigma_{\gamma_2}^x \quad (8)$$

on the ground state, where $S_I^2 = \{(n + \frac{1}{2}, m + \frac{1}{2}, 0, 0) | m, n = 0, 1, 2, \dots, L - 1\}$. For an arbitrary 1-cube, say $(\frac{3}{2}, 1, 0, 0)$ inside S_I^2 , we can easily check that $W(S_I^2)$ acts on two nearest spins at $(\frac{3}{2}, \frac{1}{2}, 0, 0)$ and $(\frac{3}{2}, \frac{3}{2}, 0, 0)$, so there will be no excited $B_{(\frac{3}{2}, 1, 0, 0)}^l$. While for $\gamma_1 = (\frac{1}{2}, 0, 0, 0)$ on the boundary of S_I^2 , since $W(S_I^2)$ only acts on one nearest spin (at $(\frac{1}{2}, \frac{1}{2}, 0, 0)$), so two $B_{(\frac{1}{2}, 0, 0, 0)}^l$ terms will be excited. Immediately after applying $W(S_I^2)$ on the ground state, we apply

$$W(S_{II}^2) = \prod_{\gamma_2 \in S_{II}^2} \sigma_{\gamma_2}^x, \quad (9)$$

where $S_{II}^2 = \{(h + \frac{1}{2}, 0, k + \frac{1}{2}, 0) | h, k = 1, 2, \dots, L - 1\}$. For $\gamma_1 = (\frac{1}{2}, 0, 0, 0) \in \partial S_I^2 \cap \partial S_{II}^2$, there will be still two excited $B_{(\frac{1}{2}, 0, 0, 0)}^l$ terms, which are respectively $B_{(\frac{1}{2}, 0, 0, 0)}^{(\hat{x}_1, \hat{x}_2, \hat{x}_4)}$ and $B_{(\frac{1}{2}, 0, 0, 0)}^{(\hat{x}_1, \hat{x}_3, \hat{x}_4)}$.

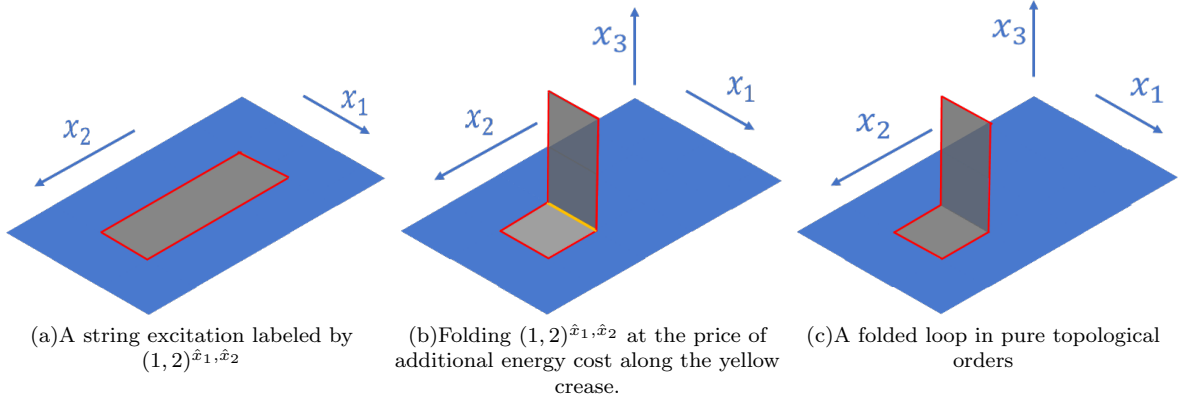


FIG. 7. A $(1, 2)^{\hat{x}_1, \hat{x}_2}$ -type excitation cannot freely escape from the plane \hat{x}_1 - \hat{x}_2 . (a) A string excitation (marked by the red line) with restricted mobility and deformability, labeled by $(1, 2)^{\hat{x}_1, \hat{x}_2}$. By applying proper local operators, a part of the string moves to \hat{x}_1 - \hat{x}_3 plane but at the unavoidable localized energy price along the crease line in yellow in (b), which leads to the deformability restriction. Alternatively speaking, the state in (b) is no longer a single-string excitation. It is similar to moving a single fracton, where the consequence is to arrive at a state with multiple fractons. For comparison, if (a) is produced in pure topological order, (a) can be deformed to (c) such that the shape of a loop is gradually and freely deformed out of the plane.

D. Complex excitations in the model-[1, 2, 3, 4]

1. Chairons of 12 flavors

In the above discussions, we have analyzed three types of simple excitations in the model-[1, 2, 3, 4]: fractons $(0, 0)$, volumeons $(0, 3)$, and strings $(1, 2)$. All these excitations belong to the category of “simple excitations” (E^s) as they are just simple geometric objects like points and strings. Surprisingly, we find that in the model-[1, 2, 3, 4], there also exist complex excitations (E^c) whose geometric structure is quite fruitful and is absent in the X-cube model in 3D. As mentioned above, the excited state in Fig. 7(b) is obtained by folding the string excitation $(1, 2)^{\hat{x}_1, \hat{x}_2}$ at the price of additional energy cost. As a matter of fact, the resulting shape in Fig. 7(b) with both red and yellow lines can be considered as a complex excitation. It is called “chairon” due to its “chair” shape. As the chairon example in Fig. 7(b) demonstrates, the most remarkable feature of complex excitations is that the energy is not distributed along manifold-like objects. For instance, when we consider a convergence of yellow and red lines in Fig. 7(b), it’s obvious that the bifurcation of lines can’t be homeomorphous to a 1D Euclidean space [85]. Therefore, we can’t simply label such an excitation by “string” or “loop”, as a result of their non-manifold nature. Originated from the different flavors of $(1, 2)$ -type excitations, chairons can also carry different flavors. By direct calculation, we can find that there are $4 \times \binom{3}{2} = 12$ flavors of chairons in total in the model-[1, 2, 3, 4].

Let us focus on the chairon in Fig. 7(b) and concretely carry out the stabilizer operators whose eigenvalues are flipped and then discuss its consequences. For all 1-cubes γ_1 along the red line within \hat{x}_1 - \hat{x}_2 plane, $B_{\gamma_1}^{(\hat{x}_1, \hat{x}_2, \hat{x}_3)} =$

$-1, B_{\gamma_1}^{(\hat{x}_1, \hat{x}_2, \hat{x}_4)} = -1$. For all 1-cubes γ_1 along the red line within \hat{x}_1 - \hat{x}_3 plane, $B_{\gamma_1}^{(\hat{x}_1, \hat{x}_2, \hat{x}_3)} = -1, B_{\gamma_1}^{(\hat{x}_1, \hat{x}_3, \hat{x}_4)} = -1$. For all 1-cubes γ_1 along the yellow crease line C^1 , $B_{\gamma_1}^{(\hat{x}_1, \hat{x}_2, \hat{x}_4)} = -1, B_{\gamma_1}^{(\hat{x}_1, \hat{x}_3, \hat{x}_4)} = -1$. these operators form the set $\{\hat{O}\}_{\text{complex}}$. Since only two operators per γ_1 along the yellow line are excited, one may conclude that energy density along the yellow line is still $2K$. As a result, energy is uniformly distributed along both yellow and red lines.

The mobility and deformability of chairons are relatively difficult to be described, in contrast to simple excitations where the integer m is good enough. According to our discussion on the mobility and deformability of $(1, 2)$ -type excitations, the two U-shaped segments (i.e., red lines in Fig. 7(b)) of a chairon are freely deformable within the 2D planes where they are located at without additional energy cost, as long as their lengths stay the same. But the deformability of the crease line is kind of unspeakable, as its length and shape are both related to the deformation of the U-shaped segments. As a whole, the chairon can move along the direction of the crease line. However, regarding a chairon as an one-dimensional excitation would be an oversimplification of its mobility and deformability for sure.

2. Yuons of 4 flavors

Except for chairons, we also find another kind of complex excitations in the model-[1, 2, 3, 4], which can be dubbed as “yuon”, since a yuon is a Y-shaped object composed of three U-shaped strings, as shown in Fig. 8. A yuon can be excited by further acting $W(S_{III}^2)$ after applying $W(S_I^2)$ and $W(S_{II}^2)$ in Eq. (8) and Eq. (9), where $S_{III}^2 = \{(n + \frac{1}{2}, 0, 0, m + \frac{1}{2}) | m, n = 0, 1, 2, \dots, L -$

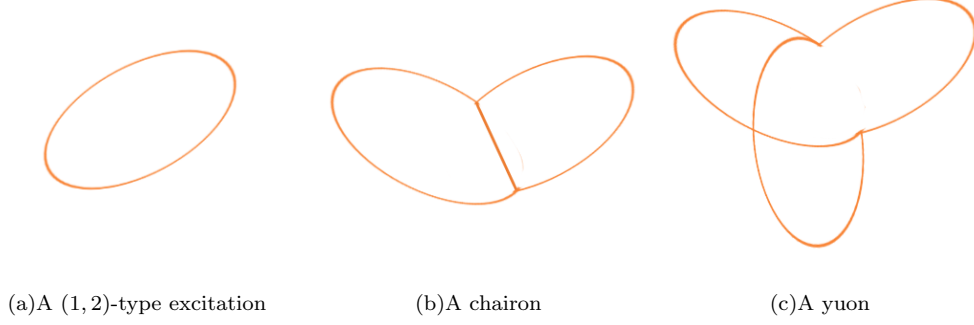


FIG. 8. Pictorial comparison among a (1, 2)-type excitation, a chairon and a yuon in the model-[1, 2, 3, 4].

1}. Although no B term along the convergence line would be excited now, as we've already applied 3 operators on the ground state, three connected U-shaped excitations will still remain, which forms a yuon. Therefore, the space that can embed a yuon must be at least four dimensional. A schematic comparison among an (1, 2)-type excitation, a chairon and a yuon in the model-[1, 2, 3, 4] is given in Fig. 8. Similar to chairons, we find that there are 4 flavors of yuons in the model-[1, 2, 3, 4].

Since chairons and yuons have already covered all kinds of intersection of (1, 2)-type excitations, we expect these two kinds of excitations can be regarded as the most elementary building blocks for all kinds of complex excitations in the model-[1, 2, 3, 4]. In Sec. IV C, we will discuss about the model-[1, 2, 3, 5], which has different kinds of "building blocks".

E. Excited states with multiple spatially separate loops in the model-[1, 2, 3, 4]

In the model-[1, 2, 3, 4] discussed here, we may discuss an excited state with multiple spatially separate loops each of which has 6 flavor options. Some typical excited states with two or three loops are listed in Table V. There are several remarks on this table:

- In pure Abelian topological order, the fusion of two loops doesn't depend on where the two loops are initially located. Case 0 demonstrates the fusion in a pure \mathbb{Z}_2 topological order. But in fracton topological order, Table V shows three different cases for the two-loop fusion due to the (partial) restriction of mobility and deformability in the model-[1, 2, 3, 4].
- In Sec. III B, we have studied an excited state with lineons ℓ_x and ℓ_y in the 3D X-cube model (i.e., the model-[0, 1, 2, 3]). If the two lineons are able to meet at some point, the fusion output is another lineon labeled by ℓ_z that can move along the straight line that is along z -direction and passes the intersection point. Nevertheless, in the Case 3,

two loops that are able to meet can only fuse to a chairon that has a connected non-manifold shape, rather than another new loop.

- We will see shortly in Sec. IV C, in the model-[0, 1, 2, 4], two lineons, if located properly, will fuse into a fracton rather than another lineon.

F. Gravity analog: energy density and spacetime curvature

In lattice of arbitrary dimension higher than 3, as our argument doesn't rely on specific dimensions, we would expect our results still persist. That is to say, a $[D-3, D-2, D-1, D]$ model would contain $(0, 0)$ -type, $(0, D-1)$ -type and $(D-3, D-2)$ -type excitations. More excitations in $[D-3, D-2, D-1, D]$ models for $D=3, 4, 5$ are listed in Table II. Moreover, in higher dimensional cases, there are similar situations that when we act $F^{D-2}(C^{D-3}) = \prod_{\gamma_{D-2} \in S_I^{D-2}} \sigma_{\gamma_{D-2}}^x \prod_{\gamma_{D-2} \in S_{II}^{D-2}} \sigma_{\gamma_{D-2}}^x$, where $S_I^{D-2} \cap S_{II}^{D-2} = \partial S_I^{D-2} \cap \partial S_{II}^{D-2} = C^{D-3}$, $B_{\gamma_{D-3}}^l$ terms along C^{D-3} will be excited for certain l 's. Such a phenomenon naturally reminds us of gravity, considering that there are already some works concerning about this problem. [30, 31] Especially, in the 6-dimensional model [3, 4, 5, 6], when the scale considered is much larger than the lattice constant, we would see condensations of flat closed 4-manifolds in the ground state. When we gradually heat up the system, energy density will rise where the 4-manifolds curve. Nevertheless, despite the direct correspondence between curvature and energy density, the curvature which matters here is extrinsic curvature, while in general relativity the correspondence is between intrinsic curvature and stress-energy tensor. As a result, the relation between our lattice models and gravity is still vague.

TABLE V. Typical examples of excited states with spatially separate loops in the model-[1, 2, 3, 4]. The two loops labeled by (*) are in the same \hat{x}_1 - \hat{x}_2 plane; The two loops labeled by (**) are in different \hat{x}_1 - \hat{x}_2 planes. Case 1 to Case 4 are two-loop states in the model-[1, 2, 3, 4], while Case 5 is a three-loop state. “Case 0” is added for comparison, which happens in pure \mathbb{Z}_2 topological order.

	1st loop	2nd loop	3rd loop	Sectors	Fusion output
<i>Case 0</i>	any position	any position	×	\mathbb{I}	vacuum
<i>Case 1</i>	$(1, 2)^{\hat{x}_1, \hat{x}_2}$	$(1, 2)^{\hat{x}_1, \hat{x}_2}$ (*)	×	\mathbb{I}	vacuum
<i>Case 2</i>	$(1, 2)^{\hat{x}_1, \hat{x}_2}$	$(1, 2)^{\hat{x}_1, \hat{x}_2}$ (**)	×	\mathbf{E}^d	intrinsically disconnected
<i>Case 3</i>	$(1, 2)^{\hat{x}_1, \hat{x}_2}$	$(1, 2)^{\hat{x}_1, \hat{x}_3}$	×	\mathbf{E}^c	 : chairon
<i>Case 4</i>	$(1, 2)^{\hat{x}_1, \hat{x}_2}$	$(1, 2)^{\hat{x}_3, \hat{x}_4}$	×	\mathbf{E}^d	intrinsically disconnected
<i>Case 5</i>	$(1, 2)^{\hat{x}_1, \hat{x}_2}$	$(1, 2)^{\hat{x}_1, \hat{x}_3}$	$(1, 2)^{\hat{x}_1, \hat{x}_4}$	\mathbf{E}^c	 : yuon

IV. GENERAL CONSTRUCTION OF LATTICE MODELS

A. Lattice Hamiltonians

As our previous sections demonstrated, we can promote $(0, 1)$ -type excitations to $(i, i + 1)$ -type excitations by lifting the dimensions of all the n -cubes where spins and other operators are located at by i . Naturally, one may be curious about, if it’s possible to define spins and operators on different kinds of n -cubes, without any redundant constraints? To deal with this problem, we come up with a further generalization procedure. In this procedure, the dimension of the objects on which the operators and spins are defined, can be adjusted independently. Since we are focusing on fracton models, other than the dimensions of spins, lower-dimensional cube operators, higher-dimensional cube operators and the total space, we also need the dimension of leaf spaces to specify such a model. For instance, for the X-cube model, we have spin dimension $d_s = 1$, lower-dimensional cube operator dimension $d_n = 0$, higher-dimensional cube operator dimension $d_c = 3$, space dimension $D = 3$ and leaf dimension $d_l = 2$. Generally, it seems that we need five dimension indexes $[d_n, d_s, d_l, d_c, D]$ to specify a member in the model “family”. Given such a 5-tuple $[d_n, d_s, d_l, d_c, D]$, the Hamiltonian of the corresponding member model is:

$$H_{[d_n, d_s, d_l, d_c, D]} = -J \sum_{\{\gamma_{d_c}\}} A_{\gamma_{d_c}} - K \sum_{\{\gamma_{d_n}\}} \sum_l B_{\gamma_{d_n}}^l, \quad (10)$$

where the definition of the terms is given below:

- A $B_{\gamma_{d_n}}^l$ term is the product of z -components of the $2^{d_s - d_n} \binom{d_l - d_n}{d_s - d_n}$ spins whose coordinates are obtained by shifting $(d_s - d_n)$ coordinates of γ_{d_n} along the directions in $\mathcal{C}_{\gamma_{d_n}}^l$ by $\pm \frac{1}{2}$. Here $\mathcal{C}_{\gamma_{d_n}}^l \equiv \mathcal{L} \cap \mathcal{C}_{\gamma_{d_n}}^i$.
- An $A_{\gamma_{d_c}}$ term is the product of x -components of the $2^{d_c - d_s} \binom{d_c}{d_c - d_s}$ spins whose coordinates are obtained

by shifting $(d_c - d_s)$ coordinates of γ_{d_c} along the directions in $\mathcal{C}_{\gamma_{d_c}}^h$ by $\pm \frac{1}{2}$.

Take the model-[1, 2, 3, 4] as an example. For a given $\gamma_1 = (0, 0, 0, \frac{1}{2})$, we can see that $\mathcal{C}_{(0,0,0,\frac{1}{2})}^i = \{\hat{x}_1, \hat{x}_2, \hat{x}_3\}$, while $\mathcal{C}_{(0,0,0,\frac{1}{2})}^h = \{\hat{x}_4\}$. For the 3 leaf spaces $\langle \hat{x}_1, \hat{x}_2, \hat{x}_4 \rangle$, $\langle \hat{x}_1, \hat{x}_3, \hat{x}_4 \rangle$ and $\langle \hat{x}_2, \hat{x}_3, \hat{x}_4 \rangle$ associated with $(0, 0, 0, \frac{1}{2})$, we have $\mathcal{C}_{(0,0,0,\frac{1}{2})}^{\langle \hat{x}_1, \hat{x}_2, \hat{x}_4 \rangle} = \{\hat{x}_1, \hat{x}_2\}$, $\mathcal{C}_{(0,0,0,\frac{1}{2})}^{\langle \hat{x}_1, \hat{x}_3, \hat{x}_4 \rangle} = \{\hat{x}_1, \hat{x}_3\}$ and $\mathcal{C}_{(0,0,0,\frac{1}{2})}^{\langle \hat{x}_2, \hat{x}_3, \hat{x}_4 \rangle} = \{\hat{x}_2, \hat{x}_3\}$ respectively, so we can obtain the $B_{(0,0,0,\frac{1}{2})}^l$ as in Eq. (7). Similarly, for the 4-cube $(\frac{1}{2}, \frac{1}{2}, \frac{1}{2}, \frac{1}{2})$, $A_{(\frac{1}{2}, \frac{1}{2}, \frac{1}{2}, \frac{1}{2})}$ can be simply obtained as in Eq. (6).

In the following part of this section, we will use \mathcal{S}_c to refer to the set of the nearest spins of the d_c -cube c , \mathcal{S}_n to refer to the set of the nearest spins of the d_n -cube n , and \mathcal{S}_n^l to refer to the set of the nearest spins of the d_n -cube n inside the d_l -dimensional leaf space l (here l is associated with n). Apparently, then we have $\cup_l \mathcal{S}_n^l = \mathcal{S}_n$.

Though we are trying to make the choice of different dimension indexes independent to each other, we still need to respect some orders of the dimensions. Firstly, we find that d_n and d_c can’t be equal to d_s , otherwise the cube operators would be trivialized. Besides, according to the dimension order of X-cube model, we expect d_n to be smaller than d_s while d_c should be larger than d_s . Furthermore, $d_l > d_s$, $d_l < D$ and $d_c \leq D$ are obviously required. However, it should be noted that the condition d_s is between d_c and d_n is not really necessary in defining an exactly solvable fracton order model. For simplicity, we will focus on cases where the condition is satisfied in this article.

Since we expect our models to be exactly solvable, we require every higher dimensional cube operator shares even or zero number of nearest spins with any lower dimensional cube operator. Since lower dimensional cube operators are embedded in different leaf spaces, this condition means that

$$|\mathcal{S}_n^l \cap \mathcal{S}_c| \bmod 2 = 0 \quad \forall l, n, c. \quad (11)$$

According to the symmetry of the cubic lattice, we can calculate $|\mathcal{S}_n^l \cap \mathcal{S}_c|$ for any pair of nearest γ_{d_n} and γ_{d_c} in the lattice. Therefore, we only need to consider the number of spins shared by

$$\gamma_{d_c} \quad c_1 = \left(\underbrace{\frac{1}{2}, \frac{1}{2}, \dots, \frac{1}{2}}_{d_c}, \underbrace{0, 0, \dots, 0}_{D-d_c} \right) \quad \text{and} \quad \gamma_{d_n} \quad n_1 = \left(\underbrace{\frac{1}{2}, \frac{1}{2}, \dots, \frac{1}{2}}_{d_n}, \underbrace{0, 0, \dots, 0}_{D-d_n} \right).$$

Apparently, for a spin s_1 that is nearest to both c_1 and n_1 , the first d_n coordinates of s_1 must be $\frac{1}{2}$ and the last $(D - d_c)$ coordinates must be 0, only the values of the $(d_c - d_n)$ coordinates in the middle are variable.

To calculate $|\mathcal{S}_n^l \cap \mathcal{S}_c|$, we only need to care about the uncertain middle part of the coordinates of s_1 , which is composed of $(d_c - d_n)$ numbers. Each subsequence consists of these $(d_c - d_n)$ numbers with $(d_s - d_n)$ digits being $\frac{1}{2}$ and the others being 0 corresponds to a spin which is simultaneously nearest to c_1 and n_1 . As a result, a shared spin will take the form $s_1 = \left(\underbrace{\frac{1}{2}, \frac{1}{2}, \dots, \frac{1}{2}}_{d_n}, \underbrace{\dots}_{d_c-d_n}, \underbrace{0, 0, \dots, 0}_{D-d_c} \right)$. For leaf l associ-

ated with n_1 , which contains α directions with uncertain coordinates (i.e. in the middle part of s_1), we have $|\mathcal{S}_{n_1}^l \cap \mathcal{S}_{c_1}| = \binom{\alpha}{d_s - d_n}$. However, as we expect the parity of $|\mathcal{S}_{n_1}^l \cap \mathcal{S}_{c_1}|$ to be independent of the choice of leaf, α should be insensitive to the choice of leaf space, which means all leaves must have the same number of uncertain digits (here we ignore the case where the change of α doesn't influence the parity of $|\mathcal{S}_{n_1}^l \cap \mathcal{S}_{c_1}|$ for simplicity). Therefore, the last part of sequence $s_1 = \left(\underbrace{\frac{1}{2}, \frac{1}{2}, \dots, \frac{1}{2}}_{d_n}, \underbrace{\dots}_{d_c-d_n}, \underbrace{0, 0, \dots, 0}_{D-d_c} \right)$ must vanish, i.e. $D - d_c$ must be 0. Then we have $\alpha = d_l - d_n \forall l$. And the exactly solvable condition is just

$$|\mathcal{S}_n^l \cap \mathcal{S}_c| \bmod 2 = \binom{d_l - d_n}{d_s - d_n} \bmod 2 = 0 \quad (12)$$

together with

$$d_n < d_s < d_l < d_c = D. \quad (13)$$

Since then, we only need a 4-tuple $[d_n, d_s, d_l, d_c]$ (or $[d_n, d_s, d_l, D]$) to specify an exactly solvable model.

B. Family tree

Based on our 4-tuple notation of models, we can understand the actual meaning of the label “[0, 1, 2, 3]” of X-cube model. With such a notation manner, we can easily obtain that X-cube is the simplest model in this series. As a result, we can use it as the starting point of a “family tree” of the generalized models, which is depicted in Fig. 1. As an example of the novel properties of the models on the tree, we will demonstrate that there are new

kinds of complex excitations in $[D - 4, D - 3, D - 2, D]$ -type of models in the next subsection. Here we would like to give a preliminary description of the ground states and energy spectrum of the models on the tree.

Because the Hamiltonian of a general model is similar to $[D - 3, D - 2, D - 1, D]$ model, which is given in Eq. (4), the ground states of a general model will obey a set of conditions of the following form:

$$A_{\gamma_{d_c}} |\phi\rangle = |\phi\rangle, \quad B_{\gamma_{d_n}}^l |\phi\rangle = |\phi\rangle \quad \forall \gamma_{d_c}, \gamma_{d-n}, l. \quad (14)$$

As always, with the σ_z -basis, we can see that every configuration is an eigenvector of an arbitrary B operator, and the total Hilbert space can be spanned by all the configurations. Furthermore, the B conditions in Eq. (14) require the eigenvalue of any B operator for all configurations in a ground state to be 1. That is to say, for any γ_{d_n} in a ground state configuration, either of the following conditions must be satisfied:

- No nearest spin is altered;
- For each pair of nearest spins linked by the γ_{d_n} , there is exactly one spin of the pair being altered (for models where $d_s - d_n \geq 2$ a “pair” should be promoted to a set of $2^{d_s - d_n}$ spins).

Then, the A condition in Eq. (14) can be seen as requiring all the ground state configurations which can be transformed to each other by acting A operators share the same weight. Therefore, we can find that the unique ground state of a general model with open boundary conditions is $|\Phi\rangle = \prod_{\gamma_{d_c}} \frac{1 + A_{\gamma_{d_c}}}{\sqrt{2}} |\uparrow\uparrow\uparrow \dots \uparrow\rangle$, where $|\uparrow\uparrow\uparrow \dots \uparrow\rangle$ refers to the reference state. Besides, please note that here the form of $A_{\gamma_{d_c}}$ also implicitly depends on d_s . With periodic boundary condition, the ground states of the tree models are expected to be degenerate. We've found signs that suggest the ground state degeneracy of these models may be more complicated than the known subextensive growth. Relevant results will be involved in our future work Ref. [87].

For models on the family tree (see Fig. 1), all simple excitations can be classified into two classes: (d_n, d_s) -type excitations and $(0, 0)$ -type excitations. Moreover, since segments of complex excitations can be regarded as the convergence of several (d_n, d_s) -type excitations, and the energy density along the segments can be determined by the number of converged (d_n, d_s) -type excitations, we only need to consider the energy cost of such convergences to determine the energy cost of a complex excitation. As in Sec. III C, here we can conclude the data of the most important simple excitations in a general model as below:

- $A_{\gamma_{d_c}} = -1$ excitations, $(0, 0)$ -type, generated by $\prod_{\gamma_{d_s} \in D^{d_c - d_s}} \sigma_{\gamma_{d_s}}^z$. The excitations sit on the vertices of the $D^{d_c - d_s}$.

- $B_{\gamma_{d_n}}^l = -1$ excitations, (d_n, d_s) -type, generated by $\prod_{\gamma_{d_s} \in S^{d_s}} o_{\gamma_{d_s}}^x$. The excitations sit on the boundary of S^{d_s} .

As for the energy cost, simply we can find that the energy cost of such a $(0,0)$ -type excitation is always J , so the energy cost of different groups of fractons are respectively $2J, 4J, \dots, 2^{d_c-d_s-1}J$. Most of the groups are fractons, except for the last one which are $(0, d_s+1)$ -type excitations (or disconnected excitations).

The spectrum of convergences of (d_n, d_s) -type excitations (i.e. segments of complex excitations) is more difficult to calculate. Generally, for a specific γ_{d_n} n_1 , we can find that the number of excited $B_{n_1}^l$ operators is determined by the number of pairs of spins around the n_1 which contain exactly one altered spin. For simplicity, such a pair will be regarded as “excited”. Therefore, we can label a convergence of (d_n, d_s) -type excitations at n_1 as an i -convergence, where i is the number of excited pairs linked by n_1 . As an i -convergence always has the same energy as a $\binom{d_l-d_n}{d_s-d_n} - i$ -convergence, we only need to consider $i \leq \lfloor \frac{d_l-d_n}{2} \rfloor$ in this article. Since there are $\binom{d_c-d_n}{d_s-d_n}$ pairs of spins linked by a given γ_{d_n} , and a leaf always contains $\binom{d_l-d_n}{d_s-d_n}$ such pairs, we can see that the energy cost of an i -convergence is just the number of different combinations of $\binom{d_l-d_n}{d_s-d_n}$ pairs (i.e. leaves) which contain odd number of excited pairs. For a given i we can find that there are $\sum_{x=0}^{\lfloor \frac{i-1}{2} \rfloor} \binom{i}{2x+1} \binom{\binom{d_c-d_n}{d_s-d_n} - i}{\binom{d_l-d_n}{d_s-d_n} - 2x - 1}$ such combinations, so the energy cost of an i -convergence on a γ_{d_n} is:

$$E_i = \sum_{x=0}^{\lfloor \frac{i-1}{2} \rfloor} \binom{i}{2x+1} \binom{\binom{d_c-d_n}{d_s-d_n} - i}{\binom{d_l-d_n}{d_s-d_n} - 2x - 1} K. \quad (15)$$

For instance, we can consider the the model-[1, 2, 3, 5]. Since $\frac{d_l-d_n}{2} = \frac{5}{2} \geq 2$, there is only one kind of convergences of $(1,2)$ -type excitations need to be discussed, that is the 2-convergences. For instance, $(\frac{1}{2}, 0, 0, 0, 0)$ links 4 pairs of spins, $(\frac{1}{2}, \pm\frac{1}{2}, 0, 0, 0)$, $(\frac{1}{2}, 0, \pm\frac{1}{2}, 0, 0)$, $(\frac{1}{2}, 0, 0, \pm\frac{1}{2}, 0)$ and $(\frac{1}{2}, 0, 0, 0, \pm\frac{1}{2})$, while a leaf like $\langle x_1, x_2, x_3 \rangle$ contains two of such pairs. So we can find that of the $\binom{5-1}{3-1} = 6$ kinds of possible combinations of pairs, there are $\sum_{x=0}^{\lfloor \frac{2-1}{2} \rfloor} \binom{2}{2x+1} \binom{\binom{5-1}{2-1} - 2}{\binom{3-1}{2-1} - 2x - 1} = 4$ combinations that contain odd number of excited pairs, so there are 4 $B_{(\frac{1}{2}, 0, 0, 0, 0)}^l$ terms being excited. Such a 2-convergence can exist as a segment of a complex excitation (β -chairon, see Sec. IV C) in the model-[1, 2, 3, 5], and its energy cost is proportional to its length. More excitations in the model-[1, 2, 3, 5] is given in Table. VII.

C. Simple excitations in the model-[0, 1, 2, 4] and [1, 2, 3, 5]

In this subsection, we will take the two models “[0, 1, 2, 4]” and “[1, 2, 3, 5]” on the family tree to exemplify the novel properties of models outside the $[D-3, D-2, D-1, D]$ series.

Let’s start with the model-[0, 1, 2, 4]. It’s easy to check that, unlike the model-[1, 2, 3, 4], the model-[0, 1, 2, 4] doesn’t contain any spatially extended excitations, which makes its spectrum much simpler. As in the X-cube model, $(0,1)$ -type excitations, i.e., lineons, are generated at the ends of straight string operators consisted of σ^x ’s, and fractons are generated at the corners of cube (i.e. D^3) operators consisted of σ^z ’s. However, there is indeed something exotic in the model-[0, 1, 2, 4]: for example, since the model is defined on a 4-dimensional lattice, the convergence of two straight strings can only dual to another convergence, so the 2-convergence becomes a fracton. While in X-cube model, since there is a duality between plaquettes and links, the point-like excitation at such a convergence can be moved along the line perpendicular to the convergence. In some sense, due to the higher space dimension, a kind of lineons in [0, 1, 2, 3] model are frozen in the model-[0, 1, 2, 4]. Let us point out some key properties of lineons and fractons in the model-[0, 1, 2, 4] summarized in Table VI:

- All topological non-trivial excitations in [0, 1, 2, 4] are point-like (here excited states composed of discrete points are also recognized “point-like”), belonging to E^s or E^d sectors.
- In contrast to [0, 1, 2, 3], fractons can be formed by either flipping A or B stabilizers. There are one kind of fractons labeled by A , but there are six kinds of fractons labeled by B stabilizers due to the six different leaf space indices ℓ^9 .
- *Two lineons can fuse into a fracton.* There are four types of lineons that can move along parallel straight lines of $\hat{x}_1, \hat{x}_2, \hat{x}_3, \hat{x}_4$ orthogonal directions. Picking two different types of lineons from four (totally 6 choices), if the two straight lines where the two lineons can move intersect at some point, the two lineons fuse into a fracton with flipped stabilizers $B_{\gamma_0}^l$ where leaf space indices ℓ exactly have 6 corresponding choices. In Sec. III B, we have reviewed that, in the model-[0, 1, 2, 3], the fusion output of two lineons if they can meet from orthogonal directions is, however, another lineon.

Then we consider the the model-[1, 2, 3, 5]. The Hamiltonian of [1, 2, 3, 5] is:

$$H_{[1,2,3,5]} = -J \sum_{\{\gamma_5\}} A_{\gamma_5} - K \sum_{\{\gamma_1\}} \sum_l B_{\gamma_1}^l. \quad (16)$$

⁹ See the “Example 2” in Sec. II B.

TABLE VI. Typical examples of excitations in the model-[0, 1, 2, 4].

Excitations	Sectors	Flipped stabilizers	Creation operators
fracton: (0, 0)	E^s	A_{γ_4}	$\prod_{\gamma_1 \in D^3} \sigma_{\gamma_1}^z$
lineon: (0, 1)	E^s	$B_{\gamma_0}^l$	$\prod_{\gamma_1 \in S^1} \sigma_{\gamma_1}^x$
connected planeon: (0, 2)	E^s	A_{γ_4}	$\prod_{\gamma_1 \in D_1^1} \sigma_{\gamma_1}^z$
fracton: (0, 0)	E^s	$B_{\gamma_0}^l$	$\prod_{\gamma_1 \in S_I^1} \sigma_{\gamma_1}^x \prod_{\gamma_1 \in S_{II}^1} \sigma_{\gamma_1}^x$, where $\partial S_I^1 \cap \partial S_{II}^1 = C^0 \neq \emptyset$
disconnected planeon	E^d	A_{γ_4}	$\prod_{\gamma_1 \in D^3} \sigma_{\gamma_1}^z$

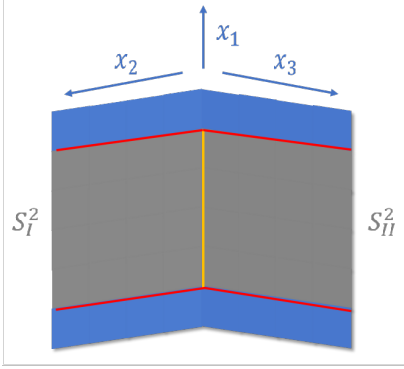


FIG. 9. A β -chairon in the model-[1, 2, 3, 5]. As in Fig. 6, here the grey plaquettes refer to spins on which a $W(S^2)$ is applied. The energy density along red lines is lower than the yellow line, according to our analysis in Sec. IV D. That is to say, energy is ununiformly distributed for a β -chairon.

The simple excitations in the model-[1, 2, 3, 5] are mostly the same as in [1, 2, 3, 4], except the mobility of groups of fractons. As basic fractons are located at the vertices of D^3 's now, pairs of fractons at the vertices of D_2^2 's become (0, 0)-type excitations, while the tetrads of fractons at the vertices of D_2^1 's belong to (0, 3)-type.¹⁰

Similar to Sec. III C, here we can classify the (1, 2)-type excitations $W(S^2)$ in the model-[1, 2, 3, 5] into $\binom{5}{2} = 10$ flavors, according to the plane (i.e. $\hat{x}_1\text{-}\hat{x}_2, \hat{x}_1\text{-}\hat{x}_3, \hat{x}_1\text{-}\hat{x}_4, \hat{x}_1\text{-}\hat{x}_5, \hat{x}_2\text{-}\hat{x}_3, \hat{x}_2\text{-}\hat{x}_4, \hat{x}_2\text{-}\hat{x}_5, \hat{x}_3\text{-}\hat{x}_4, \hat{x}_3\text{-}\hat{x}_5, \hat{x}_4\text{-}\hat{x}_5$) where S^2 is located at. Generally, when we act a $W(S^2)$ on the ground state, where S^2 is located at a $\hat{x}_i\text{-}\hat{x}_j$ plane, then at a γ_1 along the boundary of S^2 , eigenvalues of $B_{\gamma_1}^{(\hat{x}_i, \hat{x}_j, \hat{x}_k)}$, $B_{\gamma_1}^{(\hat{x}_i, \hat{x}_j, \hat{x}_h)}$ and $B_{\gamma_1}^{(\hat{x}_i, \hat{x}_j, \hat{x}_p)}$ will be flipped. Here $i, j, h, k, p \in \{1, 2, 3, 4, 5\}$, and i, j, h, k, p are all different from each other. For instance, by acting $W(S_I^2)$ on the ground state, where $S_I^2 = \{(n + \frac{1}{2}, m + \frac{1}{2}, 0, 0, 0) | m, n = 0, 1, 2, \dots, L - 1\}$, for an arbitrary γ_1 along the boundary of S_I^2 , the eigenvalue of $B_{\gamma_1}^{(\hat{x}_1, \hat{x}_2, \hat{x}_3)}$, $B_{\gamma_1}^{(\hat{x}_1, \hat{x}_2, \hat{x}_4)}$ and $B_{\gamma_1}^{(\hat{x}_1, \hat{x}_2, \hat{x}_5)}$ will be flipped. As a result,

we obtain that the energy cost of a string excitation in the model-[1, 2, 3, 5] is $3KL$, where L is the length of the string. More information of the excitations in the family tree models are summarized in Table. VI and Table. VII.

D. Complex excitations in the model-[1, 2, 3, 5] (“chairon”, “cloverion” and “xuon”)

As in the model-[1, 2, 3, 4], we can find a series of complex excitations as building blocks of general complex excitations in the model-[1, 2, 3, 5]. Some typical examples are collected in Table VII. At first, if we further apply $W(S_{II}^2)$ after $W(S_I^2)$ ($W(S_I^2)$ is given in the previous subsection), where $S_{II}^2 = \{(n + \frac{1}{2}, 0, m + \frac{1}{2}, 0, 0) | m, n = 0, 1, 2, \dots, L - 1\}$, we will have a chairon excitation, which is schematically presented in Fig. 9. Though the shape of the chairon is the same as in the model-[1, 2, 3, 4], at $(\frac{1}{2}, 0, 0, 0, 0) \in \partial S^2 \cap \partial S_{II}^2$, now we have $B_{(\frac{1}{2}, 0, 0, 0, 0)}^{(\hat{x}_1, \hat{x}_2, \hat{x}_4)}$, $B_{(\frac{1}{2}, 0, 0, 0, 0)}^{(\hat{x}_1, \hat{x}_3, \hat{x}_4)}$ and $B_{(\frac{1}{2}, 0, 0, 0, 0)}^{(\hat{x}_1, \hat{x}_3, \hat{x}_5)}$ being flipped. As now there are 4 flipped B terms at $(\frac{1}{2}, 0, 0, 0, 0)$, we can find that unlike in the model-[1, 2, 3, 4] or pure topological order, here the energy is distributed along the excitation unevenly. As a result, we can name the chairon in the model-[1, 2, 3, 4] as α -chairon, and the chairon in the model-[1, 2, 3, 5] as β -chairon, to stress their different distributions of energy. More generally, different types of chairons can be distinguished by the number of flipped stabilizers along the excitation: if the number is a constant, then we call it an α -chairon. Otherwise, it's a β -chairon. Again, by counting the possible combinations of different dimensions, we find that there are $\binom{5}{1} \times \binom{4}{2} = 30$ flavors of β -chairons in the model-[1, 2, 3, 5].

Furthermore, by acting $W(S_{III}^2)$ after $W(S_I^2)$ and $W(S_{II}^2)$, where $S_{III}^2 = \{(n + \frac{1}{2}, 0, 0, m + \frac{1}{2}, 0) | m, n = 0, 1, 2, \dots, L - 1\}$. For $\gamma_1 = (\frac{1}{2}, 0, 0, 0, 0) \in \partial S_I^2 \cap \partial S_{II}^2 \cap \partial S_{III}^2$, we will have $B_{(\frac{1}{2}, 0, 0, 0, 0)}^{(\hat{x}_1, \hat{x}_2, \hat{x}_5)}$, $B_{(\frac{1}{2}, 0, 0, 0, 0)}^{(\hat{x}_1, \hat{x}_3, \hat{x}_5)}$ and $B_{(\frac{1}{2}, 0, 0, 0, 0)}^{(\hat{x}_1, \hat{x}_4, \hat{x}_5)}$ being excited, that is to say, the 3 $W(S^2)$ operators generate a complex excitation with more complicated topology than β -chairon. But here the energy density along the excitation is uniform. Since the projection of the excitation onto a 2D plane has three “petals”, this kind of excitations can be dubbed as “cloverions”. Analogous to

¹⁰ See the “Example 3” in Sec. II B for an introduction to the leaves in model-[1, 2, 3, 5].

TABLE VII. Typical examples of excitations in the model-[1, 2, 3, 5].

Excitations	Sectors	Flipped stabilizers	Creation operators
(0, 0)	E^s	A_{γ_5}	$\prod_{\gamma_2 \in D^3} \sigma_{\gamma_2}^z$
(1, 2)	E^s	$B_{\gamma_1}^l$	$\prod_{\gamma_2 \in S^2} \sigma_{\gamma_2}^x$
connected volumeon (0, 3)	E^s	A_{γ_5}	$\prod_{\gamma_2 \in D_2^1} \sigma_{\gamma_2}^z$
β -Chairon	E^c	$B_{\gamma_1}^l$	$\prod_{\gamma_2 \in S_I^2} \sigma_{\gamma_2}^x \prod_{\gamma_2 \in S_{II}^2} \sigma_{\gamma_2}^x$, where $\partial S_I^2 \cap \partial S_{II}^2 = C^1 \neq \emptyset$
Cloverion	E^c	$B_{\gamma_1}^l$	$\prod_{\gamma_2 \in S_I^2} \sigma_{\gamma_2}^x \prod_{\gamma_2 \in S_{II}^2} \sigma_{\gamma_2}^x \prod_{\gamma_2 \in S_{III}^2} \sigma_{\gamma_2}^x$, where $\partial S_I^2 \cap \partial S_{II}^2 \cap \partial S_{III}^2 = C^1 \neq \emptyset$
Xuon	E^c	$B_{\gamma_1}^l$	$\prod_{\gamma_2 \in S_I^2} \sigma_{\gamma_2}^x \prod_{\gamma_2 \in S_{II}^2} \sigma_{\gamma_2}^x \prod_{\gamma_2 \in S_{III}^2} \sigma_{\gamma_2}^x \prod_{\gamma_2 \in S_{IV}^2} \sigma_{\gamma_2}^x$, where $\partial S_I^2 \cap \partial S_{II}^2 \cap \partial S_{III}^2 \cap \partial S_{IV}^2 = C^1 \neq \emptyset$
disconnected volumeon	E^d	A_{γ_5}	$\prod_{\gamma_2 \in D^3} \sigma_{\gamma_2}^z$

the β -chairon, we can obtain that there are $\binom{5}{1} \times \binom{4}{3} = 20$ flavors of cloverions in the model-[1, 2, 3, 5].

But unlike the model-[1, 2, 3, 4], here we can further apply $W(S_{IV}^2)$ to obtain an extra kinds of complex excitations, where $S_{IV}^2 = \{(n + \frac{1}{2}, 0, 0, 0, m + \frac{1}{2}) | m, n = 0, 1, 2, \dots, L - 1\}$. All B operators associated with $(\frac{1}{2}, 0, 0, 0, 0)$ are unflipped by the $W(S_{IV}^2)$ now, but four U-shaped strings generated by the four $W(S^2)$ operators will compose a complex excitation of a new kind. This kind of complex excitations can be dubbed as ‘‘xuon’’, as it is an X-shaped object consisted of 4 U-shaped strings. Obviously, there are only $\binom{5}{1} = 5$ flavors of xuons in the model-[1, 2, 3, 5]. A schematic comparison between β -chairons, cloverions and xuons is given in Fig. 10.

Except for [1, 2, 3, 5] and other two 5D models on the family tree (see Fig. 1)), we also have [0, 1, 4, 5], [0, 2, 4, 5] and [0, 3, 4, 5] models that are exactly solvable. Some representative excitations in more 5D models are listed in Table. VIII.

V. CONCLUDING REMARKS

In this article, we’ve demonstrated that various kinds of novel excitations can be constructed in a large class of exactly solvable models of fracton topological order, like spatially extended excitations with restricted mobility and deformability, which unveils an intriguing scenario of interplay of topology and geometry in fracton order.

There are several future directions related to fracton physics of spatially extended excitations.

1. For instance, it is worth to examine more exactly solvable instances that are outside the family tree, like [0, 1, 4, 5], [0, 2, 4, 5], [0, 3, 4, 5] model in 5D, and other 12 6D models, and discuss their properties, e.g., exotic complex excitations, fusion rules, entanglement entropy, and effective field theory.

2. As we’ve discussed in the main text, it is also interesting to explore the relation between geometry in fracton order and curved space caused by gravity.

3. By noting that volumeons denoted by (0, 3) can be constructed in some models of 4D or higher dimensions, one may conjecture that our universe may have extra dimensions while elementary particles in the Standard Model are in fact volumeons that are actually restricted inside our 3D visible space. In this sense, it is very interesting to construct a higher dimensional lattice models that support volumeons which are massive Dirac fermions! Moreover, the relationship between the existence of complex excitations and the type of the order is also an exciting question.

4. Finally, it is also interesting to study self-localization theory of spatially extended excitations with different degrees of mobility and deformability restriction.

ACKNOWLEDGMENTS

We thank Chenjie Wang, Meng Cheng, Han Ma, Hao Song, Juven Wang, Andrey Gromov, Kevin Slagle, Yizhi You, Jian-Keng Yuan, Zhi-Feng Zhang and Yuchen Ma for their beneficial communication and discussions. M.Y.L. & P.Y. were supported in part by the Sun Yat-sen University startup grant and NSFC grant no. 11847608.

[1] Xiao-Gang Wen, ‘‘A theory of 2+1d bosonic topological orders,’’ *Natl. Sci. Rev.* (2015), 10.1093/nsr/nwv077,

[arXiv:1506.05768](https://arxiv.org/abs/1506.05768).

TABLE VIII. Typical examples of excitations in more 5D models. Simple excitations are simply labeled by their mobility types in this table, so different excitations may share the same label. Names of other types of excitations are omitted for simplicity.

Models	Excitations	Sectors	Flipped stabilizers	Creation operators
[0, 1, 4, 5]	(0, 0)	E^s	A_{γ_5}	$\prod_{\gamma_1 \in D^4} \sigma_{\gamma_1}^z$
	(0, 1)	E^s	$B_{\gamma_0}^l$	$\prod_{\gamma_1 \in S^1} \sigma_{\gamma_1}^x$
		E^d	A_{γ_5}	$\prod_{\gamma_1 \in D^4} \sigma_{\gamma_1}^z$
[0, 2, 4, 5]	(0, 0)	E^s	A_{γ_5}	$\prod_{\gamma_2 \in D^3} \sigma_{\gamma_2}^z$
	(0, 0)	E^s	$B_{\gamma_0}^l$	$\prod_{\gamma_2 \in S^2} \sigma_{\gamma_2}^x$
		E^d	A_{γ_5}	$\prod_{\gamma_2 \in D^3} \sigma_{\gamma_2}^z$
[0, 3, 4, 5]	(0, 0)	E^s	A_{γ_5}	$\prod_{\gamma_3 \in D^2} \sigma_{\gamma_3}^z$
	(0, 0)	E^s	$B_{\gamma_0}^l$	$\prod_{\gamma_3 \in S^3} \sigma_{\gamma_3}^x$
		E^d	A_{γ_5}	$\prod_{\gamma_3 \in D^2} \sigma_{\gamma_3}^z$
[2, 3, 4, 5]	(0, 0)	E^s	A_{γ_5}	$\prod_{\gamma_3 \in D^2} \sigma_{\gamma_3}^z$
	(2, 3)	E^s	$B_{\gamma_2}^l$	$\prod_{\gamma_3 \in S^3} \sigma_{\gamma_3}^x$
		E^c	$B_{\gamma_2}^l$	$\prod_{\gamma_3 \in S_I^3} \sigma_{\gamma_3}^x$, where $\partial S_I^3 \cap \partial S_{II}^3 = C^2 \neq \emptyset$
		E^d	A_{γ_5}	$\prod_{\gamma_3 \in D^2} \sigma_{\gamma_3}^z$

- [2] Xiao-Gang Wen, “Topological orders in rigid states,” *International Journal of Modern Physics B* **4**, 239–271 (1990).
- [3] Chetan Nayak, Steven H. Simon, Ady Stern, Michael Freedman, and Sankar Das Sarma, “Non-abelian anyons and topological quantum computation,” *Rev. Mod. Phys.* **80**, 1083–1159 (2008).
- [4] Claudio Chamon, “Quantum glassiness in strongly correlated clean systems: An example of topological overprotection,” *Phys. Rev. Lett.* **94**, 040402 (2005).
- [5] Sagar Vijay, Jeongwan Haah, and Liang Fu, “A new kind of topological quantum order: A dimensional hierarchy of quasiparticles built from stationary excitations,” *Phys. Rev. B* **92**, 235136 (2015).
- [6] Peng Ye and Qing-Rui Wang, “Monopoles, confinement and charge localization in the t-j model with dilute holes,” *Nucl. Phys. B* **874**, 386–398 (2013).
- [7] Wilbur Shirley, Kevin Slagle, Zhenghan Wang, and Xie Chen, “Fracton models on general three-dimensional manifolds,” *Phys. Rev. X* **8**, 031051 (2018).
- [8] Sagar Vijay, Jeongwan Haah, and Liang Fu, “Fracton topological order, generalized lattice gauge theory, and duality,” *Phys. Rev. B* **94**, 235157 (2016).
- [9] Abhinav Prem, Jeongwan Haah, and Rahul Nandkishore, “Glassy quantum dynamics in translation invariant fracton models,” *Phys. Rev. B* **95**, 155133 (2017).
- [10] Wilbur Shirley, Kevin Slagle, and Xie Chen, “Foliated fracton order from gauging subsystem symmetries,” *SciPost Phys.* **6**, 41 (2019).
- [11] Han Ma, Ethan Lake, Xie Chen, and Michael Hermele, “Fracton topological order via coupled layers,” *Phys. Rev. B* **95**, 245126 (2017).
- [12] Jeongwan Haah, “Local stabilizer codes in three dimensions without string logical operators,” *Phys. Rev. A* **83**, 042330 (2011).
- [13] Daniel Bulmash and Maissam Barkeshli, “Gauging fractons: immobile non-Abelian quasiparticles, fractals, and position-dependent degeneracies,” arXiv e-prints, arXiv:1905.05771 (2019), arXiv:1905.05771 [cond-mat.str-el].
- [14] A. Prem and D. J. Williamson, “Gauging permutation symmetries as a route to non-Abelian fractons,” arXiv e-prints (2019), arXiv:1905.06309 [cond-mat.str-el].
- [15] D. Bulmash and M. Barkeshli, “Generalized $U(1)$ Gauge Field Theories and Fractal Dynamics,” arXiv e-prints (2018), arXiv:1806.01855 [cond-mat.str-el].
- [16] K. T. Tian, E. Samperton, and Z. Wang, “Haah codes on general three manifolds,” arXiv e-prints (2018), arXiv:1812.02101 [quant-ph].
- [17] Yizhi You, Daniel Litinski, and Felix von Oppen, “Higher order topological superconductors as generators of quantum codes,” arXiv e-prints, arXiv:1810.10556 (2018), arXiv:1810.10556 [cond-mat.str-el].
- [18] Han Ma, Michael Hermele, and Xie Chen, “Fracton topological order from the higgs and partial-confinement mechanisms of rank-two gauge theory,” *Phys. Rev. B* **98**, 035111 (2018).
- [19] Kevin Slagle and Yong Baek Kim, “Fracton topological order from nearest-neighbor two-spin interactions and dualities,” *Phys. Rev. B* **96**, 165106 (2017).
- [20] Gábor B. Halász, Timothy H. Hsieh, and Leon Balents, “Fracton topological phases from strongly coupled spin chains,” *Phys. Rev. Lett.* **119**, 257202 (2017).
- [21] Kevin T. Tian and Zhenghan Wang, “Generalized Haah Codes and Fracton Models,” arXiv e-prints, arXiv:1902.04543 (2019), arXiv:1902.04543 [quant-ph].
- [22] Wilbur Shirley, Kevin Slagle, and Xie Chen, “Foliated fracton order from gauging subsystem symmetries,” *SciPost Phys.* **6**, 41 (2019).

- [23] W. Shirley, K. Slagle, and X. Chen, “Fractional excitations in foliated fracton phases,” arXiv e-prints (2018), [arXiv:1806.08625 \[cond-mat.str-el\]](#).
- [24] Kevin Slagle, David Aasen, and Dominic Williamson, “Foliated Field Theory and String-Membrane-Net Condensation Picture of Fracton Order,” *SciPost Phys.* **6**, 43 (2019).
- [25] Abhinav Prem, Sheng-Jie Huang, Hao Song, and Michael Hermele, “Cage-net fracton models,” *Phys. Rev. X* **9**, 021010 (2019).
- [26] Shriya Pai, Michael Pretko, and Rahul M. Nandkishore, “Localization in fractonic random circuits,” *Phys. Rev. X* **9**, 021003 (2019).
- [27] Shriya Pai and Michael Pretko, “Dynamical scar states in driven fracton systems,” arXiv e-prints, arXiv:1903.06173 (2019), [arXiv:1903.06173 \[cond-mat.stat-mech\]](#).
- [28] Pablo Sala, Tibor Rakovszky, Ruben Verresen, Michael Knap, and Frank Pollmann, “Ergodicity-breaking arising from Hilbert space fragmentation in dipole-conserving Hamiltonians,” arXiv e-prints, arXiv:1904.04266 (2019), [arXiv:1904.04266 \[cond-mat.str-el\]](#).
- [29] Ajesh Kumar and Andrew C. Potter, “Symmetry-enforced fractonicity and two-dimensional quantum crystal melting,” *Phys. Rev. B* **100**, 045119 (2019).
- [30] Michael Pretko, “The fracton gauge principle,” *Phys. Rev. B* **98**, 115134 (2018).
- [31] Michael Pretko, “Subdimensional particle structure of higher rank $u(1)$ spin liquids,” *Phys. Rev. B* **95**, 115139 (2017).
- [32] Michael Pretko, “Generalized electromagnetism of subdimensional particles: A spin liquid story,” *Phys. Rev. B* **96**, 035119 (2017).
- [33] L. Radzihovsky and M. Hermele, “Fractons from vector gauge theory,” arXiv e-prints (2019), [arXiv:1905.06951 \[cond-mat.str-el\]](#).
- [34] A. Dua, I. H. Kim, M. Cheng, and D. J. Williamson, “Sorting topological stabilizer models in three dimensions,” arXiv e-prints (2019), [arXiv:1908.08049 \[quant-ph\]](#).
- [35] Andrey Gromov, “Chiral topological elasticity and fracton order,” *Phys. Rev. Lett.* **122**, 076403 (2019).
- [36] Jeongwan Haah, *Lattice quantum codes and exotic topological phases of matter*, Ph.D. thesis, California Institute of Technology (2013).
- [37] Andrey Gromov, “Towards classification of fracton phases: The multipole algebra,” *Phys. Rev. X* **9**, 031035 (2019).
- [38] Yizhi You, Trithap Devakul, S. L. Sondhi, and F. J. Burnell, “Fractonic Chern-Simons and BF theories,” arXiv e-prints, arXiv:1904.11530 (2019), [arXiv:1904.11530 \[cond-mat.str-el\]](#).
- [39] Juven Wang and Kai Xu, “Higher-Rank Tensor Field Theory of Non-Abelian Fracton and Embeddon,” arXiv e-prints, arXiv:1909.13879 (2019), [arXiv:1909.13879 \[hep-th\]](#).
- [40] Shriya Pai and Michael Pretko, “Fractonic line excitations: An inroad from three-dimensional elasticity theory,” *Phys. Rev. B* **97**, 235102 (2018).
- [41] Michael Pretko and Rahul M. Nandkishore, “Localization of extended quantum objects,” *Phys. Rev. B* **98**, 134301 (2018).
- [42] Dominic J. Williamson, Zhen Bi, and Meng Cheng, “Fractonic matter in symmetry-enriched $u(1)$ gauge theory,” *Phys. Rev. B* **100**, 125150 (2019).
- [43] Arpit Dua, Dominic J. Williamson, Jeongwan Haah, and Meng Cheng, “Compactifying fracton stabilizer models,” *Phys. Rev. B* **99**, 245135 (2019).
- [44] Bowen Shi and Yuan-Ming Lu, “Deciphering the nonlocal entanglement entropy of fracton topological orders,” *Phys. Rev. B* **97**, 144106 (2018).
- [45] Hao Song, Abhinav Prem, Sheng-Jie Huang, and M. A. Martin-Delgado, “Twisted fracton models in three dimensions,” *Phys. Rev. B* **99**, 155118 (2019).
- [46] Sagar Vijay, Jeongwan Haah, and Liang Fu, “Fracton topological order, generalized lattice gauge theory, and duality,” *Phys. Rev. B* **94**, 235157 (2016).
- [47] Michael Pretko, Xie Chen, and Yizhi You, “Fracton Phases of Matter,” arXiv e-prints, arXiv:2001.01722 (2020), [arXiv:2001.01722 \[cond-mat.str-el\]](#).
- [48] Alioscia Hamma, Paolo Zanardi, and Xiao-Gang Wen, “String and membrane condensation on three-dimensional lattices,” *Phys. Rev. B* **72**, 035307 (2005).
- [49] Tian Lan, Liang Kong, and Xiao-Gang Wen, “Classification of $(3+1)$ D bosonic topological orders: The case when pointlike excitations are all bosons,” *Phys. Rev. X* **8**, 021074 (2018).
- [50] Tian Lan and Xiao-Gang Wen, “Classification of $3+1$ D bosonic topological orders (ii): The case when some pointlike excitations are fermions,” *Phys. Rev. X* **9**, 021005 (2019).
- [51] Liang Kong and Xiao-Gang Wen, “Braided fusion categories, gravitational anomalies, and the mathematical framework for topological orders in any dimensions,” (2014), unpublished, [arXiv:1405.5858](#).
- [52] AtMa P. O. Chan, Peng Ye, and Shinsei Ryu, “Braiding with borromean rings in $(3+1)$ -dimensional spacetime,” *Phys. Rev. Lett.* **121**, 061601 (2018).
- [53] Xueda Wen, Huan He, Apoorv Tiwari, Yunqin Zheng, and Peng Ye, “Entanglement entropy for $(3+1)$ -dimensional topological order with excitations,” *Phys. Rev. B* **97**, 085147 (2018).
- [54] Chenjie Wang and Michael Levin, “Braiding statistics of loop excitations in three dimensions,” *Phys. Rev. Lett.* **113**, 080403 (2014).
- [55] Chao-Ming Jian and Xiao-Liang Qi, “Layer construction of 3d topological states and string braiding statistics,” *Phys. Rev. X* **4**, 041043 (2014).
- [56] Shenghan Jiang, Andrej Mesaros, and Ying Ran, “Generalized modular transformations in $(3+1)$ D topologically ordered phases and triple linking invariant of loop braiding,” *Phys. Rev. X* **4**, 031048 (2014).
- [57] Chenjie Wang, Chien-Hung Lin, and Michael Levin, “Bulk-boundary correspondence for three-dimensional symmetry-protected topological phases,” *Phys. Rev. X* **6**, 021015 (2016).
- [58] Yidun Wan, Juven C. Wang, and Huan He, “Twisted gauge theory model of topological phases in three dimensions,” *Phys. Rev. B* **92**, 045101 (2015).
- [59] Peng Ye, Taylor L. Hughes, Joseph Maciejko, and Eduardo Fradkin, “Composite particle theory of three-dimensional gapped fermionic phases: Fractional topological insulators and charge-loop excitation symmetry,” *Phys. Rev. B* **94**, 115104 (2016).
- [60] Peng Ye and Zheng-Cheng Gu, “Topological quantum field theory of three-dimensional bosonic abelian-

- symmetry-protected topological phases,” *Phys. Rev. B* **93**, 205157 (2016).
- [61] A. Kapustin and R. Thorngren, “Anomalies of discrete symmetries in various dimensions and group cohomology,” ArXiv e-prints (2014), [arXiv:1404.3230 \[hep-th\]](https://arxiv.org/abs/1404.3230).
- [62] Peng Ye and Xiao-Gang Wen, “Constructing symmetric topological phases of bosons in three dimensions via fermionic projective construction and dyon condensation,” *Phys. Rev. B* **89**, 045127 (2014).
- [63] Shang-Qiang Ning, Zheng-Xin Liu, and Peng Ye, “Symmetry enrichment in three-dimensional topological phases,” *Phys. Rev. B* **94**, 245120 (2016).
- [64] S.-Q. Ning, Z.-X. Liu, and P. Ye, “Topological gauge theory, symmetry fractionalization, and classification of symmetry-enriched topological phases in three dimensions,” arXiv e-prints (2018), [arXiv:1801.01638 \[cond-mat.str-el\]](https://arxiv.org/abs/1801.01638).
- [65] Peng Ye, “Three-dimensional anomalous twisted gauge theories with global symmetry: Implications for quantum spin liquids,” *Phys. Rev. B* **97**, 125127 (2018).
- [66] Juven C. Wang and Xiao-Gang Wen, “Non-abelian string and particle braiding in topological order: Modular $SL(3, \mathbb{Z})$ representation and $(3+1)$ -dimensional twisted gauge theory,” *Phys. Rev. B* **91**, 035134 (2015).
- [67] Juven C. Wang, Zheng-Cheng Gu, and Xiao-Gang Wen, “Field-theory representation of gauge-gravity symmetry-protected topological invariants, group cohomology, and beyond,” *Phys. Rev. Lett.* **114**, 031601 (2015).
- [68] Xiao Chen, Apoorv Tiwari, and Shinsei Ryu, “Bulk-boundary correspondence in $(3+1)$ -dimensional topological phases,” *Phys. Rev. B* **94**, 045113 (2016).
- [69] J. Wang, X.-G. Wen, and S.-T. Yau, “Quantum Statistics and Spacetime Surgery,” ArXiv e-prints (2016), [arXiv:1602.05951 \[cond-mat.str-el\]](https://arxiv.org/abs/1602.05951).
- [70] Pavel Putrov, Juven Wang, and Shing-Tung Yau, “Braiding statistics and link invariants of bosonic/fermionic topological quantum matter in $2+1$ and $3+1$ dimensions,” *Annals of Physics* **384**, 254 – 287 (2017).
- [71] Peng Ye, Meng Cheng, and Eduardo Fradkin, “Fractional s -duality, classification of fractional topological insulators, and surface topological order,” *Phys. Rev. B* **96**, 085125 (2017).
- [72] Apoorv Tiwari, Xiao Chen, and Shinsei Ryu, “Wilson operator algebras and ground states of coupled BF theories,” *Phys. Rev. B* **95**, 245124 (2017).
- [73] Kevin Walker and Zhenghan Wang, “ $(3+1)$ -TQFTs and topological insulators,” *Frontiers of Physics* **7**, 150–159 (2012), [arXiv:1104.2632 \[cond-mat.str-el\]](https://arxiv.org/abs/1104.2632).
- [74] Alexei Kitaev, “Periodic table for topological insulators and superconductors,” *AIP Conference Proceedings* **1134**, 22–30 (2009), <https://aip.scitation.org/doi/pdf/10.1063/1.3149495>.
- [75] Andreas P. Schnyder, Shinsei Ryu, Akira Furusaki, and Andreas W. W. Ludwig, “Classification of topological insulators and superconductors in three spatial dimensions,” *Phys. Rev. B* **78**, 195125 (2008).
- [76] Xiao-Liang Qi, Taylor L. Hughes, and Shou-Cheng Zhang, “Topological field theory of time-reversal invariant insulators,” *Phys. Rev. B* **78**, 195424 (2008).
- [77] Shinsei Ryu, Andreas P Schnyder, Akira Furusaki, and Andreas W W Ludwig, “Topological insulators and superconductors: tenfold way and dimensional hierarchy,” *New Journal of Physics* **12**, 065010 (2010).
- [78] Xie Chen, Zheng-Cheng Gu, Zheng-Xin Liu, and Xiao-Gang Wen, “Symmetry protected topological orders and the group cohomology of their symmetry group,” *Phys. Rev. B* **87**, 155114 (2013).
- [79] Xie Chen, Yuan-Ming Lu, and Ashvin Vishwanath, “Symmetry-protected topological phases from decorated domain walls,” *Nature Communications* **5**, 3507 EP – (2014).
- [80] Matthew F. Lapa, Chao-Ming Jian, Peng Ye, and Taylor L. Hughes, “Topological electromagnetic responses of bosonic quantum hall, topological insulator, and chiral semimetal phases in all dimensions,” *Phys. Rev. B* **95**, 035149 (2017).
- [81] Shauna Kravec, John McGreevy, and Brian Swingle, “All-fermion electrodynamics and fermion number anomaly inflow,” *Phys. Rev. D* **92**, 085024 (2015).
- [82] Shang-Qiang Ning, Zheng-Xin Liu, and Peng Ye, “Topological gauge theory, symmetry fractionalization, and classification of symmetry-enriched topological phases in three dimensions,” arXiv e-prints , [arXiv:1801.01638](https://arxiv.org/abs/1801.01638) (2018), [arXiv:1801.01638 \[cond-mat.str-el\]](https://arxiv.org/abs/1801.01638).
- [83] Chao-Ming Jian and Cenke Xu, “Interacting topological insulators with synthetic dimensions,” *Phys. Rev. X* **8**, 041030 (2018).
- [84] Lukasz Fidkowski, Jeongwan Haah, and Matthew B. Hastings, “An Exactly Solvable Model for a $4 + 1D$ Beyond-Cohomology Symmetry Protected Topological Phase,” arXiv e-prints , [arXiv:1912.05565](https://arxiv.org/abs/1912.05565) (2019), [arXiv:1912.05565 \[cond-mat.str-el\]](https://arxiv.org/abs/1912.05565).
- [85] Tohru Eguchi, Peter B. Gilkey, and Andrew J. Hanson, “Gravitation, gauge theories and differential geometry,” *Physics Reports* **66**, 213 – 393 (1980).
- [86] Stephen Boyd and Lieven Vandenbergh, “Mathematical background,” in *Convex Optimization* (Cambridge University Press, 2004) p. 631652.
- [87] Meng-Yuan Li and Peng Ye, “In progress.”

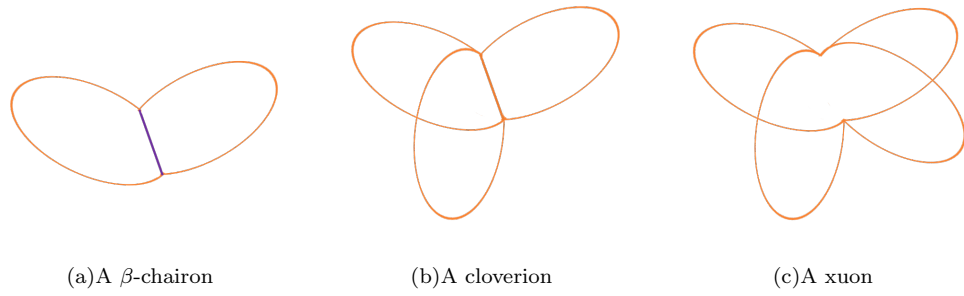


FIG. 10. Pictorial comparison among a β -chairon, a cloverion and a xuon in the model-[1, 2, 3, 5]. The crease line with higher energy density in β -chairon is highlighted with purple.